SEVERE WIND HAZARD ASSESSMENT QUEENSLAND

Technical Report Two: Hazard assessment for future climate scenarios in Queensland

Evaluating the impact of climate change on tropical cyclone-related extreme winds

Queensland Government

Australian Government
Geoscience Australia

CYCLONE TESTING STATION

Authors

Craig Arthur and Umma Zannat, Geoscience Australia

Dr Ralph Trancoso and Jozef Syktus, Department of Environment and Science

Additional contributions acknowledged throughout.

Acknowledgements

This project would not have been possible without:

The tireless efforts of Geoscience Australia to pursue the best available information to improve the understanding of tropical cyclone risk in Queensland and more broadly across Australia.

The Queensland Department of Environment and Science's Science Delivery and Knowledge Division for determined efforts and collaboration on the climate change analysis and development of all associated resources.

James Cook University's Cyclone Testing Station for contributions.

The National Computational Infrastructure Facility for providing the computing resources to develop and analyse the scenarios. The resources provided enabled the project to complete the development of the catalogue in minimal time, and also permitted interactive analysis and scenario selection.

For further information on the Hazard assessment for future climate scenarios in Queensland, please contact:

The Hazard and Risk Unit, Queensland Fire and Emergency Services	Community Safety Branch, Geoscience Australia
Email: hazard.risk@qfes.qld.gov.au Telephone: (07) 3635 3042	Email: hazards@ga.gov.au Telephone: 1800 800 173

Sources for the images used in this document:

- Front and back covers – Source: National Aeronautics and Space Administration
- Inside front cover – Source: Austock
- Introduction – Source: Austock
- Current understanding of tropical cyclone wind hazard – Source: Austock
- Projections of tropical cyclone wind hazard – Source: Dreamtime
- Hazard maps for Queensland – Source: Dreamtime
- Projections of hazard profiles for communities – Source: Dreamtime
- Summary title page – Source: Dreamtime
- Inside back cover – Source: Dreamtime

Bibliographic reference: Queensland Fire and Emergency Services and Geoscience Australia, 2022.
Severe Wind Hazard Assessment for Queensland. Technical Report Two: An evaluation of current and future tropical cyclone risk. Queensland Fire and Emergency Services, Brisbane. Geoscience Australia, Canberra.
https://www.disaster.qld.gov.au/qermf/Pages/Assessment-and-plans.aspx.

Contents

1 Introduction 8

2 Current understanding of tropical cyclone wind hazard 10

2.1 Hazard profiles for communities 12

2.2 Hazard maps for Queensland 16

3 Projections of tropical cyclone wind hazard 18

3.1 Developing projections of tropical cyclone wind hazard 19

3.2 Frequency 22

3.2.1 Trends in frequency 23

3.3 Intensity 24

3.4 Landfall 26

4 Hazard maps for Queensland 29

4.1 1% annual exceedance probability wind speeds 30

4.2 0.2% annual exceedance probability wind speed maps 35

4.3 Changes in hazard 40

5 Projections of hazard profiles for communities 44

6 Summary 50

7 References 52

Appendix A: Acronyms 54

Appendix B: Annual recurrence intervals and event probability 55

Appendix C: Likely impacts of near-future tropical cyclones on the Great Barrier Reef 57

Figures

Figure 1: Graph showing the number of severe and non-severe tropical cyclones from 1970-2020 which have occurred in the Australian region. Severe tropical cyclones are shown here as those with a minimum central pressure less than 970 hPa. Source: Geoscience Australia and Bureau of Meteorology 11

Figure 2: TC wind hazard profile for Gold Coast. 13

Figure 3: TC wind hazard profile for Gladstone. 13

Figure 4: TC wind hazard profile for Mackay. 14

Figure 5: TC wind hazard profile for Townsville. 14

Figure 6: TC wind hazard profile for Cairns. 15

Figure 7: TC wind hazard profile at Kowanyama. 15

Figure 8: 100-year ARI wind speed map for Queensland. 16

Figure 9: 500-year ARI wind speed for Queensland. 17

Figure 10: 2000-year ARI wind speed for Queensland. 17

Figure 11: Simulation domain used for hazard calculation and the landfall gates used in later analysis. The track domain is not shown. 20

Figure 12: Lifetime maximum intensity (LMI) of TCLVs (using the scaled intensity) versus long-term daily mean potential intensity at the location of LMI for the suite of 11 regional climate models. 21

Figure 13: Projected frequency of TCLVs in the suite of 11 RCMs for the future period 2081-2100. 22

Figure 14: Trends in TCLV frequency for the groups of models (rows) and the emission scenarios (columns). 23

Figure 15: Distribution of maximum intensity (wind speeds, m/s) for combinations of model ensemble groups and emission pathways. 24

Figure 16: Trends in maximum wind speed quantiles. 25

Figure 17: Latitude of lifetime maximum intensity for the ensembles and RCP pathways. 26

Figure 18: TC landfall rates for Queensland coastline for reference and future time periods. These landfall rates are based on 10,000 simulated years of TC activity for each time period. 27

Figure 19: Relative change in landfall rates for future time periods compared to the reference period (1981-2010). 27

Figure 20: Relative change in landfall rates for severe TCs (Category 3-5) for future time periods, compared to the reference period (1981-2010). None of the changes are considered statistically significant. 28

Figure 21: 1% AEP wind speed for Queensland, for the period 1981-2020. 30

Figure 22: 1% AEP wind speed for Queensland, for the period 2021-2040. 31

Figure 23: 1% AEP wind speed for Queensland, for the period 2041-2060. 32

Figure 24: 1% AEP wind speed for Queensland, for the period 2061-2080. 33

Figure 25: 1% AEP wind speed for Queensland, for the period 2081-2100. 34

Figure 26: 0.2% AEP wind speed for the period 1981-2020, based on the RCM-derived TC climate. 35

Figure 27: 0.2% AEP wind speed for the period 2021-2040, based on the RCM-derived TC climate. 36

Figure 28: 0.2% AEP wind speed for the period 2041-2060, based on the RCM-derived TC climate. 37

Figure 29: 0.2% AEP wind speed for the period 2061-2080, based on the RCM-derived TC climate. 38

Figure 30: 0.2% AEP wind speed for the period 2081-2100, based on the RCM-derived TC climate. 39

Figure 31: Change in 0.2% AEP wind speed for Queensland for the period 2021-2040. 40

Figure 32: Change in 0.2% AEP wind speed for Queensland for the period 2041-2060. 41

Figure 33: Change in 0.2% AEP wind speed for Queensland for the period 2061-2080. 42

Figure 34: Change in 0.2% AEP wind speed for Queensland for the period 2081-2100. 43

Figure 35: Annual exceedance probability curves for Gold Coast. 45

Figure 36: Annual exceedance probability curves for Gladstone. 46

Figure 37: Annual exceedance probability curves for Mackay. 47

Figure 38: Annual exceedance probability curves for Townsville. 47

Figure 39: Annual exceedance probability curves for Cairns. 48

Figure 40: Annual exceedance probability curves for Kowanyama. 49

Figure 41: Probability of one or more events with a defined exceedance probability, given a specified time span for occurrence of events. 55

Figure 42: Great Barrier Reef modelled exposure to tropical cyclone generated waves under a current climate for seven reefs spanning the length (north to south) and breadth (inner, middle, outer continental shelf position) of the region. The top two rows show the modelled duration of waves capable of damaging most coral colonies under common conditions (10 year return period – top row) versus rare conditions (100 year return period – 2nd row). The bottom two rows show the modelled maximum significant wave height (Hs- average of top 1/3 highest waves) for common conditions (10 year return period – 3rd row) versus rare conditions (100 year return period – bottom row). 59

Figure 43: High resolution (10 metre) bathymetry data for seven selected reefs spanning the length (north to south) and breadth (inner, middle, outer continental shelf position) of the Great Barrier Reef used in numerical modelling of cyclone wave exposure. 59

Figure 44: Great Barrier Reef modelled exposure to tropical cyclone generated waves under a near-future (2050) climate (8.5 degree scenario) for seven reefs spanning the length (north to south) and breadth (inner, middle, outer continental shelf position) of the region. The top two rows show the expected change in the modelled duration of waves capable of damaging most coral colonies under common conditions (10 year return period – top row) versus rare conditions (100 year return period – 2nd row). The bottom two rows show the expected change in the modelled maximum significant wave height (Hs- average of top 1/3 highest waves) for common conditions (10 year return period – 3rd row) versus rare conditions (100 year return period – bottom row). 60

Figure 45: Summary of key project findings for an example reef (Green Island) to eventually be provided for all 3,000 reefs of the Great Barrier Reef in a follow-up paper from this project. It shows the current exposure to cyclone waves as per Figure 119, how this is expected to change as per Figure 121, and the depth profile of the reef as per Figure 123. 61

Tables

Table 1:	Grouping of GCMs for ensemble simulations	22
Table 2:	Probability of one or more events with a defined annual exceedance probability, given a specified time span.	55
Table 3:	Average recurrence intervals for events with a defined probability of occurring once in a given time span.	56

1 INTRODUCTION

1 Introduction

Climate change is expected to influence the frequency, intensity and behaviour of tropical cyclones (TCs) globally, with most researchers agreeing there will be a global decline in TC frequency, but a shift towards more intense TCs (Knutson et al., 2020).

> *"There remains uncertainty in the future change in tropical cyclone frequency (the number of tropical cyclones in a given period) projected by climate models, with a general tendency for models to project fewer tropical cyclones in the Australia region in the future climate and a greater proportion of the high intensity storms (stronger wind speeds and heavier rainfall)."*
>
> CSIRO and Bureau of Meteorology, Climate Change in Australia, 2015

There are multiple lines of evidence suggesting long term trends in TC frequency and intensity are already observable. For example, Callaghan and Power (2011) have observed a statistically significant decline in the frequency of severe landfalling TCs at centennial scales along the Queensland coastline. Holland and Bruyère (2014) reported that global intensity distribution has "developed bimodal characteristics … growing consistently from 1965 to the present", which represents an increasing proportion of severe tropical cyclones though, regional trends are less clear.

There is greater uncertainty in the projected changes at a regional versus a global level (Knutson et al., 2020 and references therein). It is these regional changes that will influence the likelihood of TC-related extreme winds across Queensland. To quantify the changes in likelihood, we use a statistical model of tropical cyclones that can generate a large collection of tracks that are similar to the historical record of cyclones to extrapolate multiple scenarios using the historical events as a basis.

By using this model, it is possible to generate many thousands of years of TC activity, which enables us to better explore the likelihood of TC-related extreme winds. For example, there have been only 24 cyclones pass within 50km of Townsville since 1907, and the highest wind speed recorded since observations began in 1940 was 196km/h in TC Althea in 1972. Using a statistical model allows us to extend the record of TCs to many thousands of years, enabling robust calculation of the likelihood of extreme winds.

In a similar manner, we can leverage the information extracted from regional climate models to inform the evaluation of the likelihood of extreme TC-related winds. Details on the approach are described briefly in this report, and will be reported in detail in subsequent scientific publications. In this analysis, there is no translation to impacts, as there are no reliable projections for building exposure and vulnerability for the future time periods examined here. Thus, it is not possible to develop a holistic view of the estimated future *impacts* of TCs on Queensland communities as was demonstrated in *Severe Wind Hazard Assessment for Queensland Technical Report One*, which evaluates modelled current and future tropical cyclone impacts.

2 CURRENT UNDERSTANDING OF TROPICAL CYCLONE WIND HAZARD

2 Current understanding of tropical cyclone wind hazard

Tropical cyclones in the Australian region are influenced by several factors, and in particular variations in the El Niño – Southern Oscillation. In general, more TCs cross the coast during La Niña years, and fewer during El Niño years.

Analysis of historical TC data has limitations due to several changes in observing practices and technology that have occurred over time. With new and improved meteorological satellites our ability to detect TCs has improved, as has our ability to differentiate TCs from other tropical weather systems such as monsoon depressions, which in the past may have been incorrectly named as TCs. A particularly important change occurred in the late 1970s when regular satellite images became first available from geostationary satellites above the Earth's equator.

The time series of analysed TC activity in the Australian region (south of the equator; 90-160°E) show that the total number of TCs appears to have decreased. However, there was a change to the definition for TCs in 1978 which led to some systems which would previously have been classified as TCs instead being considered sub-tropical systems. The trend in the total number of all tropical cyclones from 1985 onwards shows no significant change.

The number of severe TCs (minimum central pressure less than 970 hPa) is dominated by variability with periods of lower and higher frequencies of occurrence. There is less confidence in the earlier intensity data with continuous satellite coverage commencing in 1979.

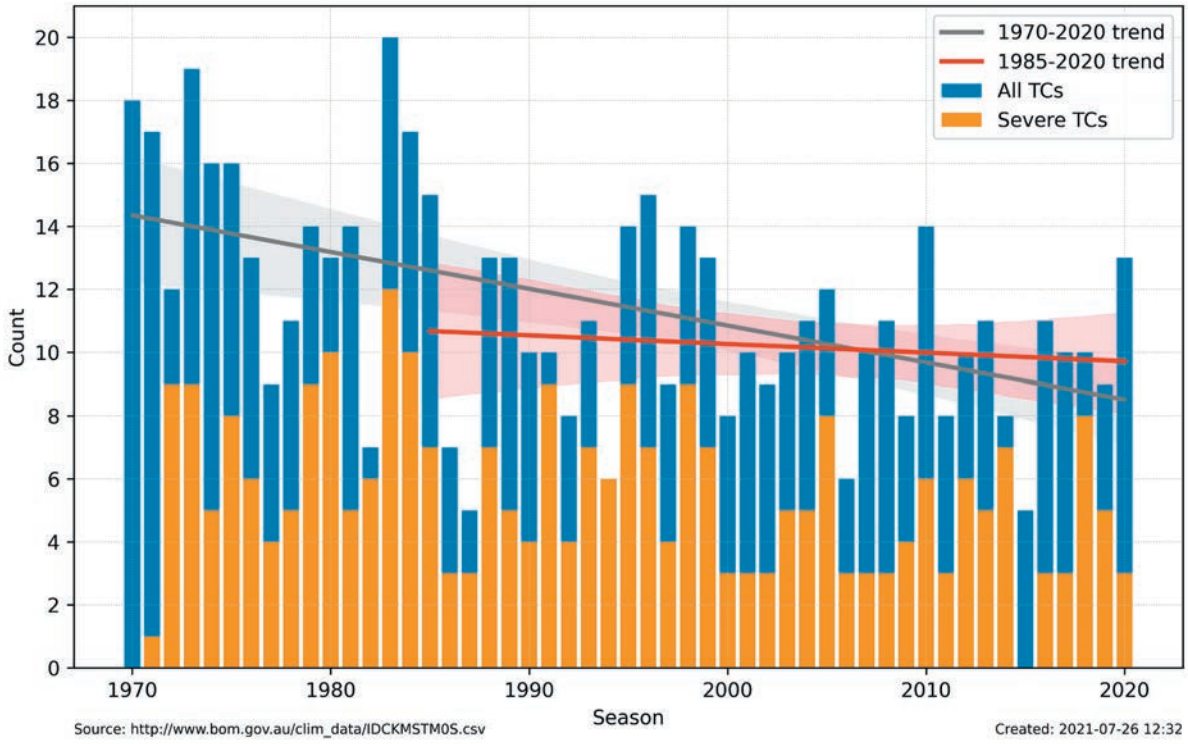

Figure 1: Graph showing the number of severe and non-severe tropical cyclones from 1970-2020 which have occurred in the Australian region. Severe tropical cyclones are shown here as those with a minimum central pressure less than 970 hPa. Source: Geoscience Australia and Bureau of Meteorology

The current modelled TC wind hazard (as described in Technical Report 1) is a modification to the 2018 Tropical Cyclone Hazard Assessment (TCHA) undertaken by Geoscience Australia (Arthur, 2018). The modification includes updates to the radius to maximum winds regression model and landfall decay model, and correcting the translation speed implementation. These modifications result in the reduction of the occurrence of large storms, hazard levels inland and far field winds. The hazard describes the likelihood of extreme wind speeds and can be presented as return periods (or average recurrence intervals) or as annual exceedance probabilities. The TC wind hazard model used a stochastic TC model to simulate 10,000 years of TC activity, thereby creating a synthetic record of TCs from which we can infer the likelihood of extreme winds.

The modelled current wind hazard was developed using the observed record of TC activity, as maintained by the Bureau of Meteorology. There is evidence that there are centennial or longer fluctuations in TC activity in northern Queensland (Nott and Hayne, 2001; Nott et al., 2009), but given the absence of quantitative data on the tracks of these prehistoric events, this information was not considered. These studies may provide a further reference for the potential extrema in TC activity (both frequency and intensity) along the Queensland coast under past climate conditions.

2.1 Hazard profiles for communities

To communicate the potential impacts of severe tropical cyclones across the diverse region of Queensland, we selected seven communities of Queensland that are representative of the differences in climatology, demographics, social vulnerability and regional economic profiles.

These are:

- **Complex Urban Environment (SEQ):** City of Gold Coast
- **Complex Urban Environment (NQ):** Townsville and surrounding region
- **Regional Economic Centre:** Gladstone and Mackay
- **Tourism Centre:** Cairns and the surrounding region
- **Remote Indigenous Communities:** Kowanyama and Pormpuraaw

These communities align with those identified in the Severe Wind Hazard Assessment for Queensland (SWHA-Q) *Technical Report One: An evaluation of current and future tropical cyclone risk* (Arthur et al. 2020).

For this assessment, we present modelled hazard profiles – illustrated in the following figures – for six of the seven communities in the form of annual recurrence interval (ARI) curves. No modelled TC wind hazard profile was extracted for Pormpuraaw, as there was no weather station located in the community. Similar curves are available for 195 locations across the simulation domain. This information can be requested from Geoscience Australia.

For each of the modelled hazard profiles below, we have used an empirical estimation of the ARI:

$$ARI = \frac{1}{\left(1 - F_x(x)\right)/n_{obs}}$$

where $F_x(x)$ is the empirical cumulative distribution function and $n_{obs} = 365.25$ is the average number of observations per year. Each point in the curve represents the modelled wind speed at the location of an individual simulated event from the 10,000 year catalogue.

The modelled hazard profiles are for TC-related wind speeds only. In South East Queensland, the modelled hazard profile is also influenced by thunderstorm-related winds, which are likely to dominate the profile at shorter recurrence intervals. That is, wind speeds from thunderstorms are likely to be greater than those for TCs.

Across all the locations, the recurrence interval of Category 4-5 winds (greater than 63m/s) is very low – the recurrence interval is generally over 1,000 years. Please note this interval is for individual locations; the cumulative likelihood of these wind speeds *anywhere* over Queensland is much higher.

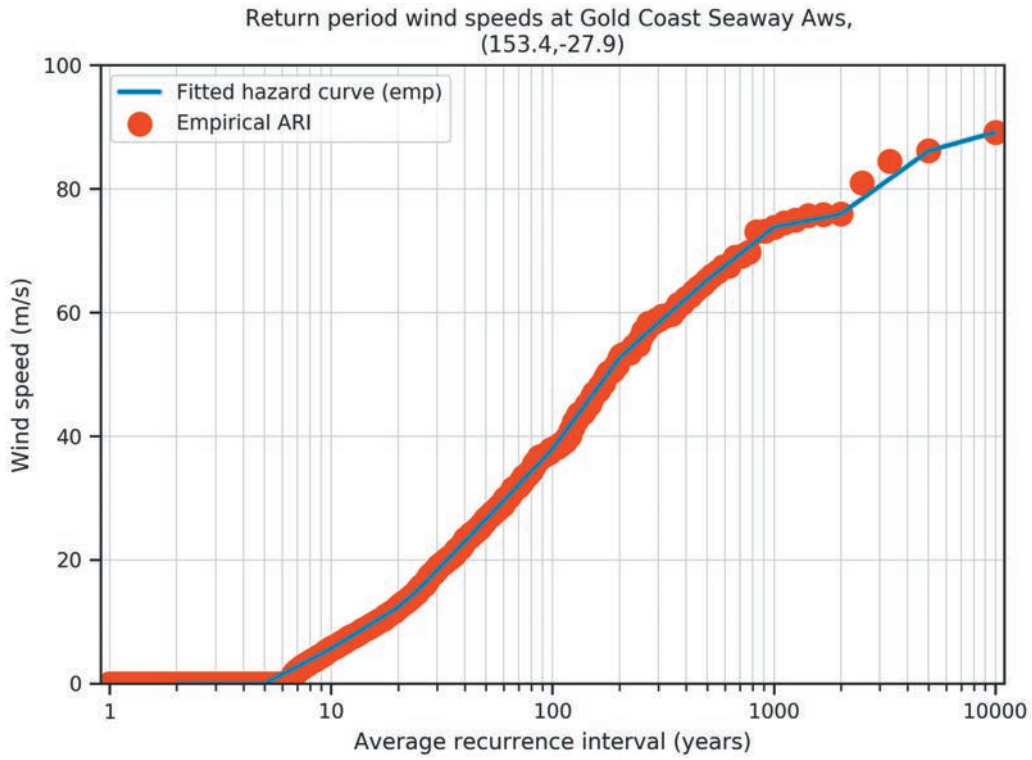

Figure 2: Modelled TC wind hazard profile for Gold Coast.

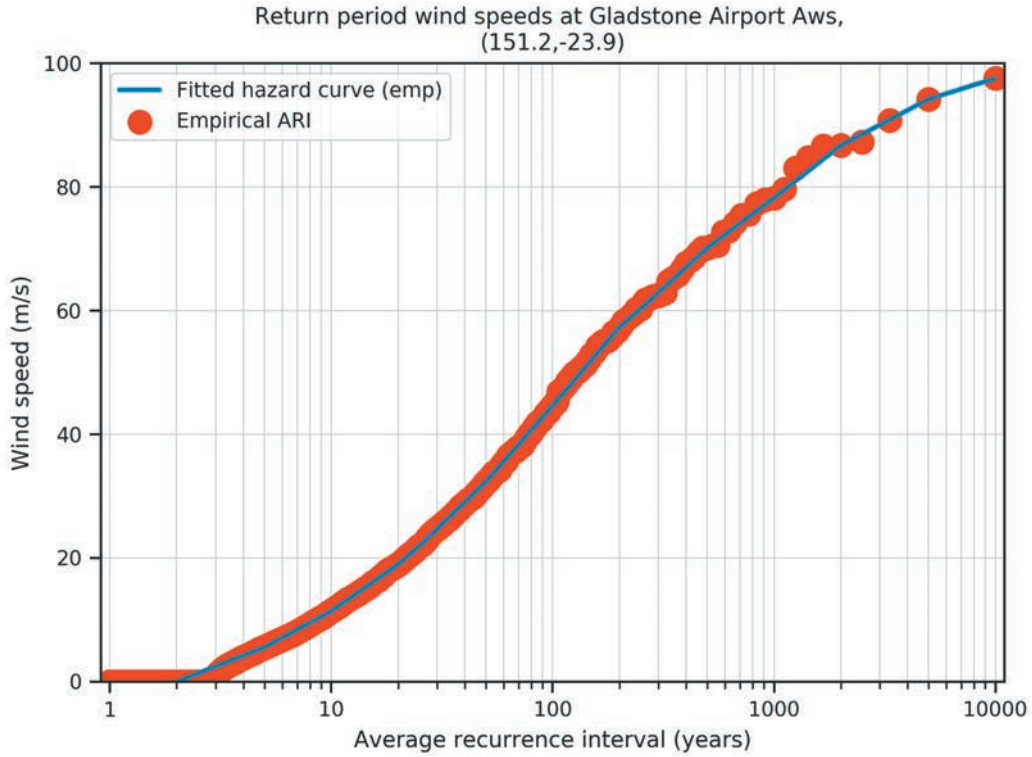

Figure 3: TC wind hazard profile for Gladstone.

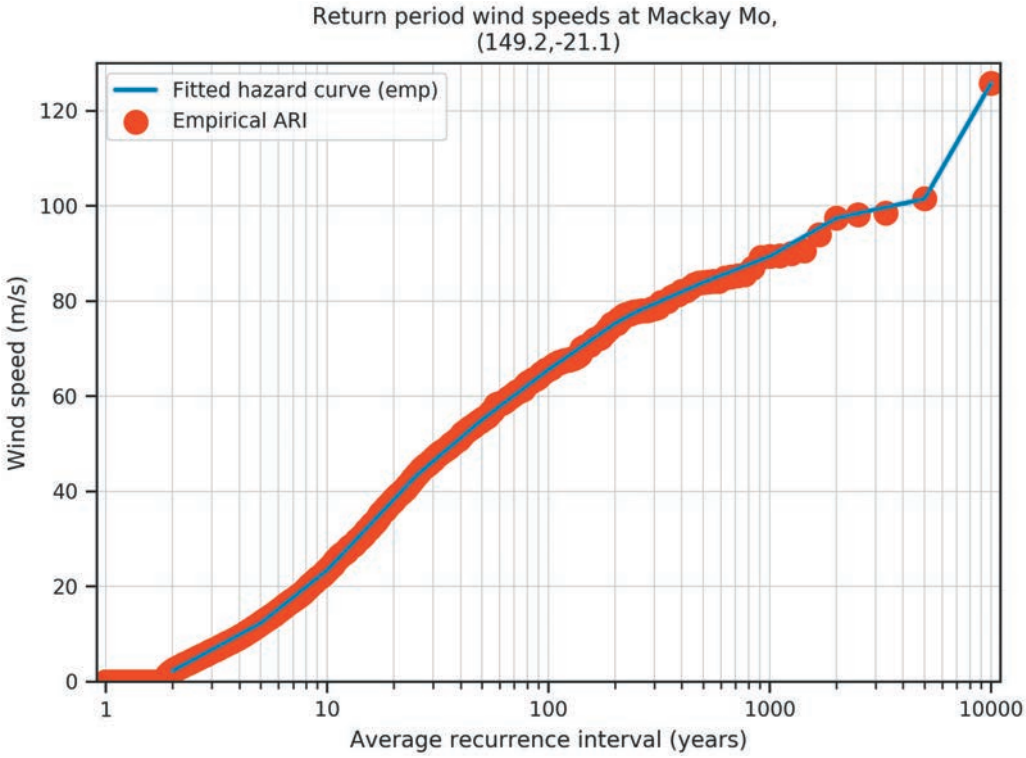

Figure 4: TC wind hazard profile for Mackay.

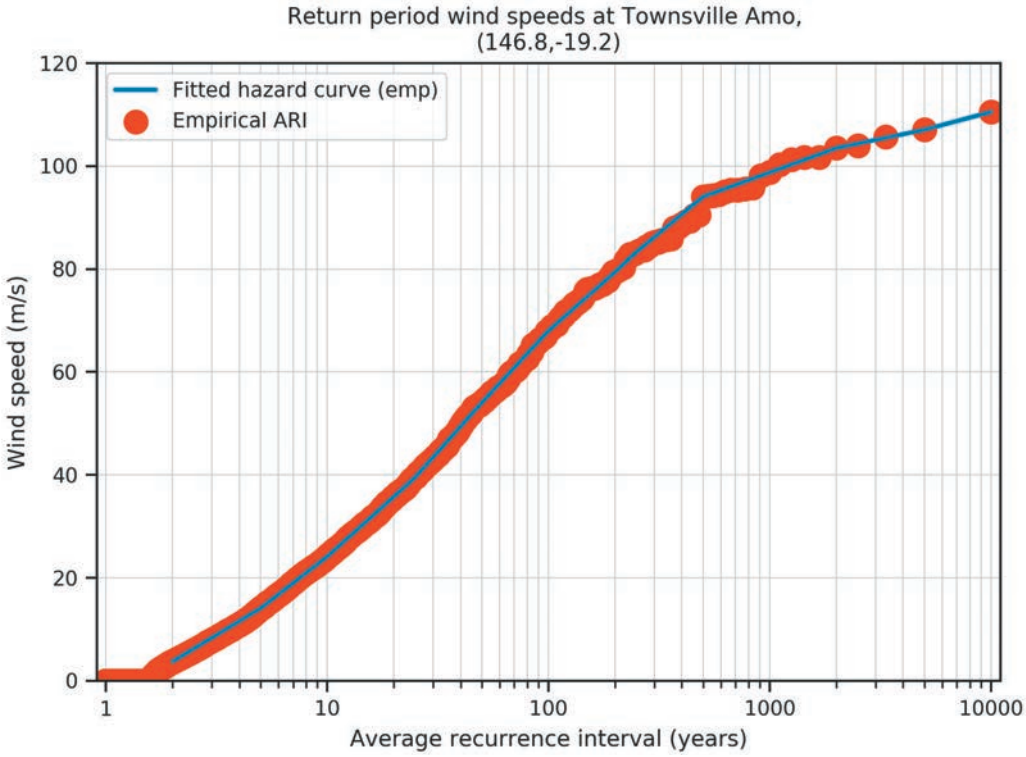

Figure 5: TC wind hazard profile for Townsville.

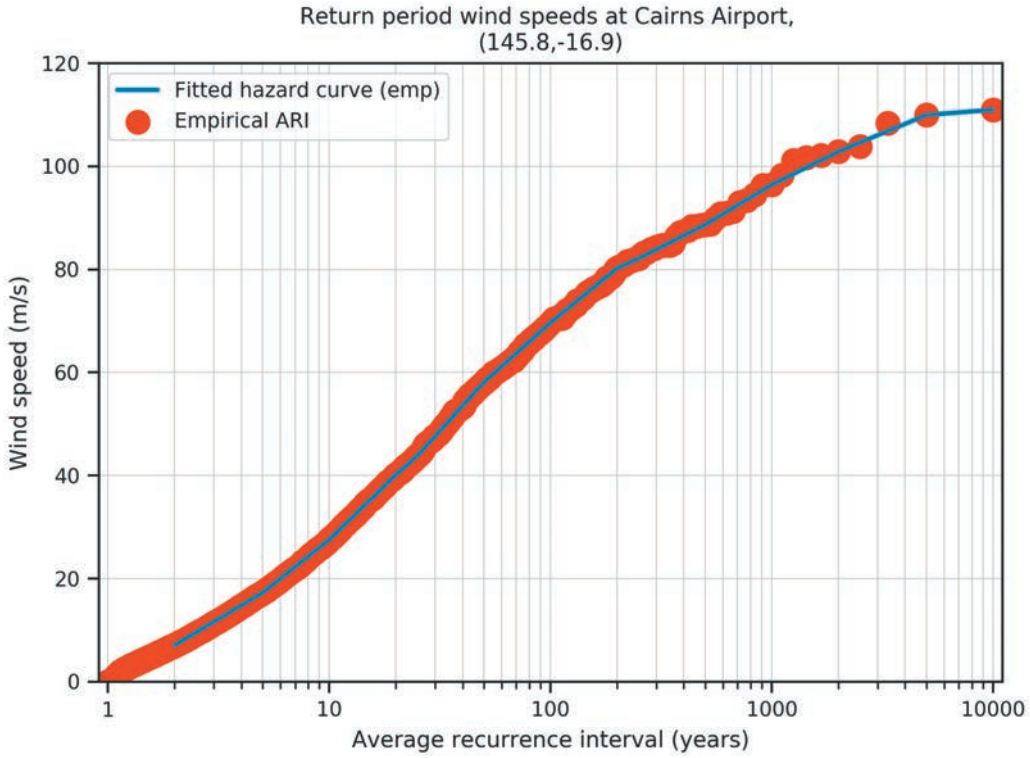

Figure 6: TC wind hazard profile for Cairns.

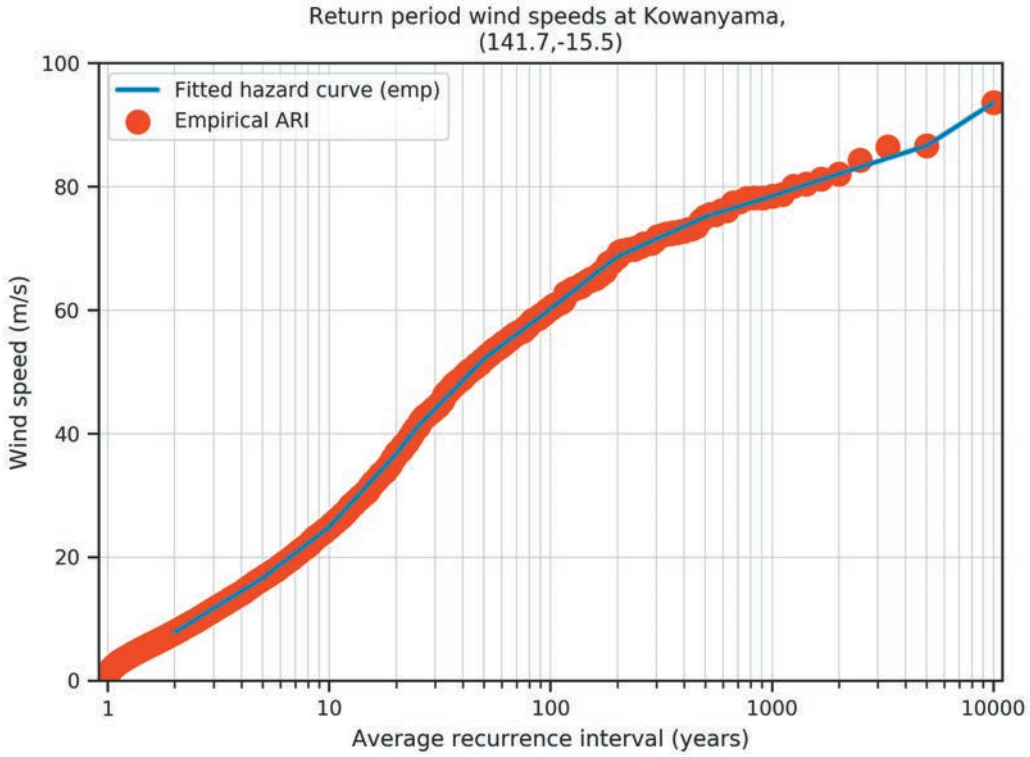

Figure 7: TC wind hazard profile at Kowanyama.

2.2 Hazard maps for Queensland

The current understanding of TC wind hazard is presented in the form of average recurrence interval wind speed maps. For a fixed recurrence interval (or return period), a location with a higher return period wind speed has a greater hazard. The maps are derived by calculating the probability of different wind speeds from a catalogue of a large number of years of simulated TC activity.

The 100-year ARI wind speed (shown in Figure 8) corresponds to a 1% annual exceedance probability – that is, there is approximately a 1% chance of that wind speed occurring in any given year. The 1% AEP wind speed corresponds to approximately a 20% probability of occurrence over a 25 year period (for more information, refer to Appendix B).

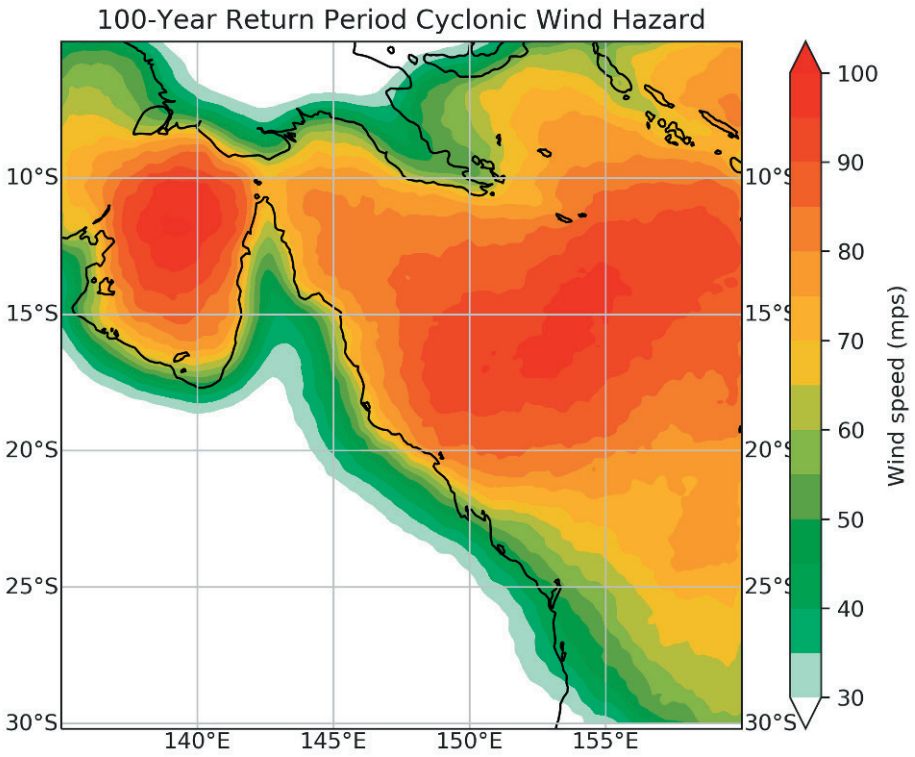

Figure 8: 100-year ARI wind speed map for Queensland.

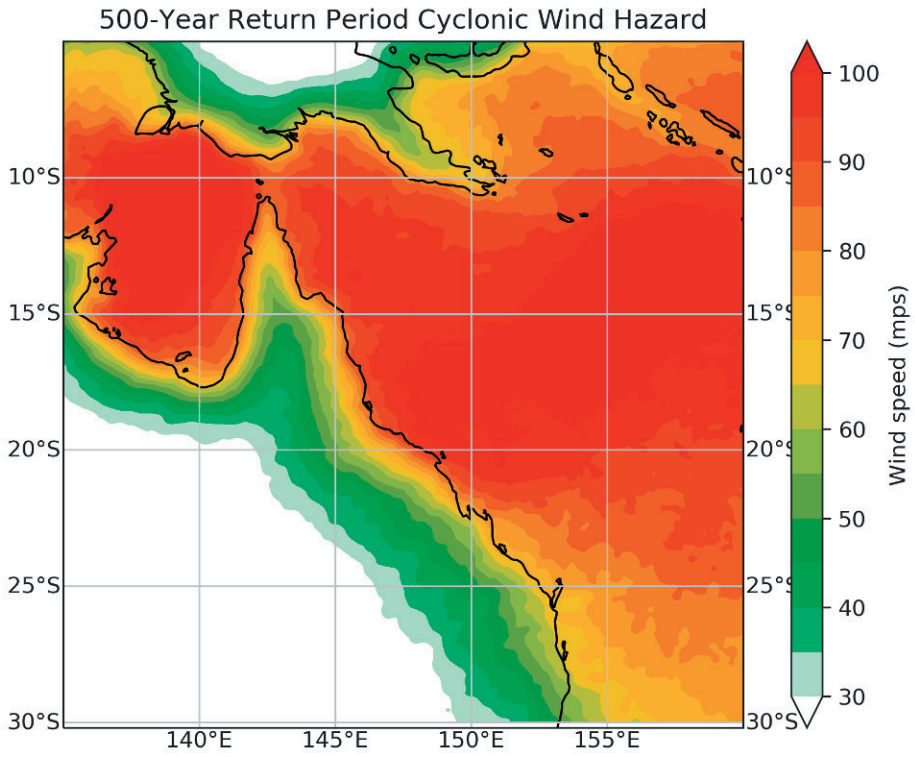

Figure 9: 500-year ARI wind speed for Queensland.

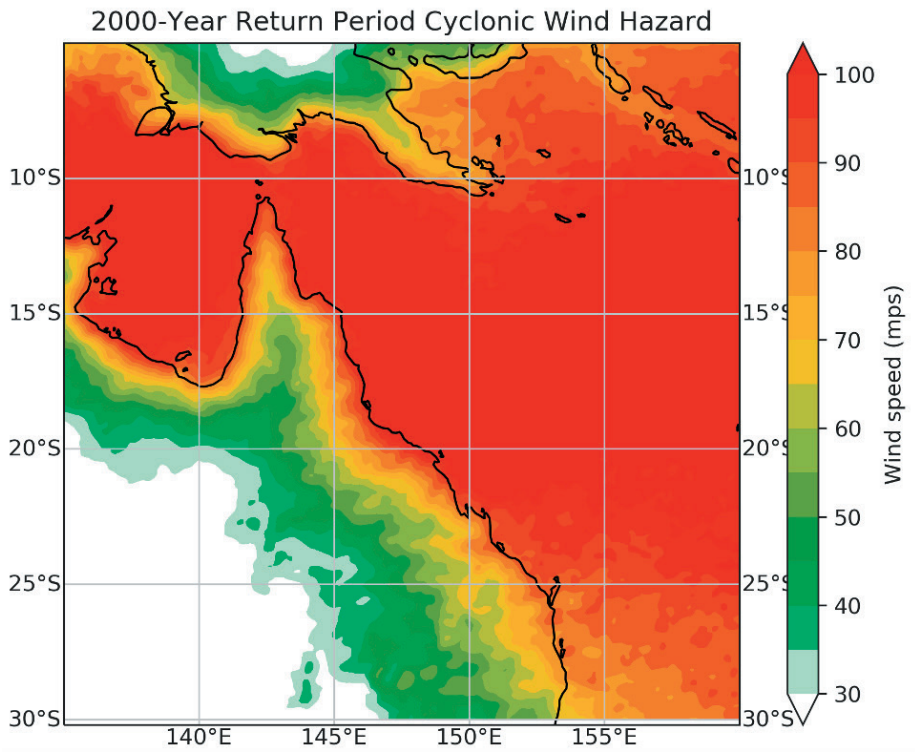

Figure 10: 2000-year ARI wind speed for Queensland.

3 PROJECTIONS OF TROPICAL CYCLONE WIND HAZARD

3 Projections of tropical cyclone wind hazard

To understand the future likelihood of extreme winds from TCs, we explored the changes in TC behaviour using downscaled climate data from CMIP5[1] general circulation models.

Notably, Schwalm et al. (2020) found that the emissions that are consistent with RCP8.5[2] are in close agreement with historical total cumulative CO_2 emissions, and that RCP8.5 is also the best match out to year 2050 under current and stated policies globally (despite many cases globally of more ambitious commitments at a national and sub-national level). As such, for quantifying physical climate risk, especially over near to midterm policy-relevant time horizons, Schwalm et al. (2020) argue for the use of RCP8.5. As such, the focus of this report is on the outcomes of the RCP8.5 scenario, with results for the RCP4.5[3] scenario described in subsequent technical papers. The modelled TC wind hazard reported in the Technical Report 1 used Geoscience Australia's Tropical Cyclone Risk Model (TCRM; Arthur, 2021) to evaluate ARI wind speeds across Australia. We use the TCRM again for evaluating ARI wind speeds but use Tropical Cyclone-Like Vortices (TCLVs) data as the input data source (Siqueira et al., 2014).

3.1 Developing projections of tropical cyclone wind hazard

We used high resolution (~10km^2) downscaled projections developed by the Queensland Government for use on their Queensland Future Climate portal and its Queensland Future Climate Dashboard. The Queensland Government modelling was performed with CSIRO's Conformal-Cubic Atmospheric Model (CCAM; McGregor and Dix, 2008; Thatcher and McGregor, 2011). CCAM is an atmospheric model forced by bias-corrected sea surface temperature (SST) data (Hoffmann et al., 2016), with no coupling between the atmosphere and oceans. Eleven CMIP5 general circulation models were selected for downscaling with two emission scenarios – RCP4.5 and RCP8.5 – representing moderate and high emissions scenarios respectively (Syktus et al., 2020). These projections have been evaluated for extreme events and shown spatially similar patterns with observational data (Trancoso et al., 2020; Eccles et al., 2020). The CCAM data was regridded to ~30km spatial resolution over the Queensland region and CSIRO's direct detection method was used to identify TC tracks.

We recognise the shortcomings of not using a coupled atmosphere-ocean model (Ogata et al., 2016) and note this issue should be addressed in future TC hazard modelling activities. Critically, Ogata et al. (2016) and Zarzycki (2016) both found that incorporating atmosphere-ocean coupling reduced the intensity of the most intense TCs (at least for General Circulation Models [GCMS]), which would have profound impacts on the likelihood of extreme wind speeds viewed from the perspective of ARIs. However, recently both coupled atmosphere-ocean and atmospheric only climate simulations with CCAM were completed over the Australian region. The results show small reductions in TCLV numbers and intensity in coupled atmosphere-ocean simulations. Therefore, we conclude that both coupled atmosphere-ocean and atmospheric only climate simulations produce similar TC characteristics.

Hence, the findings presented here represent the best-available information on modelled TC wind hazard across Queensland using high resolution downscaled projections. The information in this analysis presents a first attempt at quantifying the changing hazard profile, and can be used to describe the potential future that may need to be prepared for. It also identifies areas that should be the focus of further research.

TCLVs were extracted from CCAM data using the CSIRO direct detection and tracking algorithm (Walsh, 1997; Nguyen and Walsh, 2001), adapting the thresholds for the resolution of the downscaled simulations (Walsh and Syktus, 2003; Walsh et al., 2004; Walsh et al., 2007; Walsh et al., 2013). The algorithm works by identifying features in the climate model output that resemble TCs, based on elements such as:

- a surface pressure minimum
- a warm central core
- high cyclonic vorticity in the proximity of the surface pressure minimum, and
- rotation of winds about the central point of the system.

[1] Coupled Model Intercomparison Project Phase 5: https://www.wcrp-climate.org/wgcm-cmip/wgcm-cmip5.

[2] Representative Concentration Pathway – emission scenarios used in climate modelling that provide plausible descriptions of the future with respect to a range of variables, including greenhouse gas emissions (van Vuuren et al., 2011). RCP8.5 refers to an emission pathway where radiative forcing from greenhouse gases reaches a level of 8.5 W/m^2 by 2100.

[3] RCP4.5 refers to an emission pathway where radiative forcing from greenhouse gases reaches a level of 4.5 W/m^2 by 2100.

The detection and tracking algorithm provides information on the location and intensity of TCLVs, which can be used as an equivalent dataset to observed tracks for input into stochastic hazard models.

The track domain is defined by the extent of all events that enter the region bounded by 135°E – 160°E, 5°S – 30°S at some stage in their lifetime. This captures events with an extent that spans much of Australia and the South West Pacific Ocean (once the complete tracks are accounted for). Wind fields are only for those events that enter the simulation domain (or pass within a predefined distance of the domain).

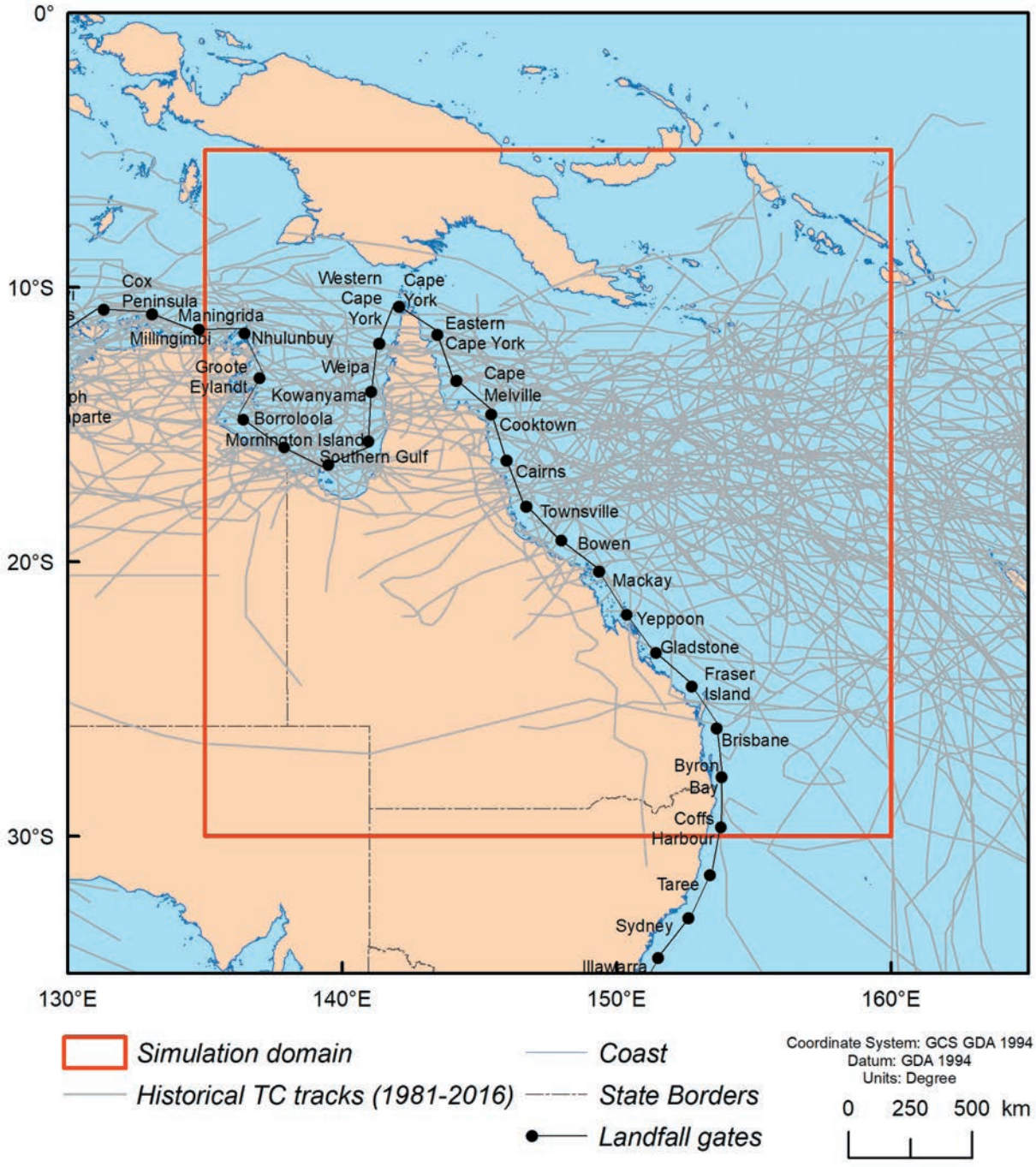

Figure 11: Simulation domain used for hazard calculation. Also shown are the landfall gates used in later analysis. The track domain is not shown.

Intensity of TCLVs (measured by central pressure deficit) was scaled using quantile delta mapping (Cannon et al., 2015) to ensure the distribution of intensity of TCLVs in the reference period (1981-2010) matched the observed distribution from historical records. Quantile delta mapping allows us to scale the intensity of future climate TCLVs in a way that ensures the relationship between quantiles in the reference period and the future periods is conserved. This can allow for events in the projected climate to attain intensities not observed in the historical record. The scaled intensity is compared to thermodynamic intensity constraints ('potential intensity') to ensure the procedure does not create a physically inconsistent intensity distribution (Figure 12).

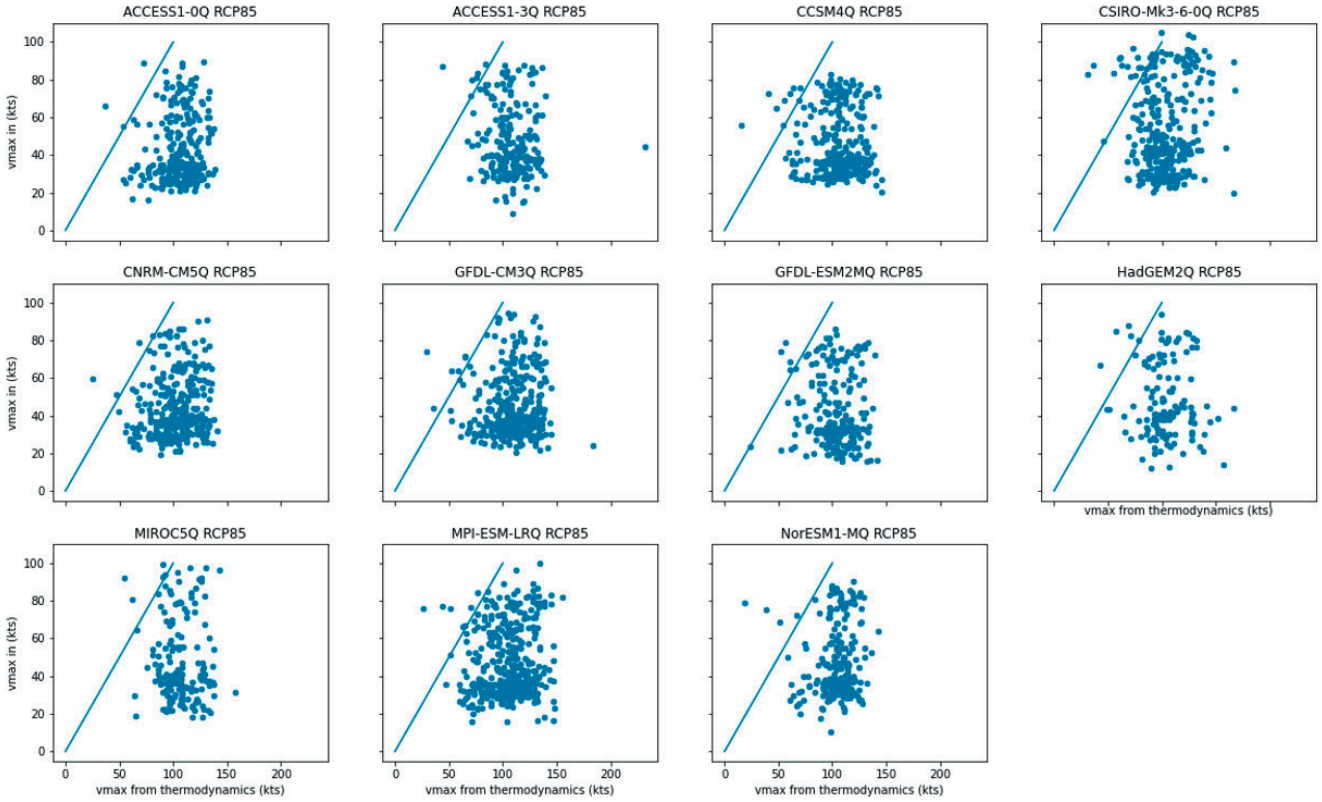

Figure 12: Lifetime maximum intensity (LMI) of TCLVs (using the scaled intensity) versus long-term daily mean potential intensity at the location of LMI for the suite of 11 regional climate models. Points above and to the left of the solid line indicate events where the LMI exceeds the potential intensity. In each case, the potential intensity (PI) values are calculated from the parent regional climate model.

In an effort to ensure the hazard projections are based on sufficient records of input data, we merge the models into two ensembles. Individually, each model provides 20 years of TCLV data for each projection period (and 30 years for the reference period 1981-2010). Such a short record can result in a paucity of data to derive track statistics suitable for the stochastic track generation process, especially in the later projection periods where the frequency of events for some individual models is very low – the HadGEM2 (refer to Table 1) model has only 15 events for the 20-year period 2018-2100 in the RCP8.5 simulation. By aggregating into these ensembles, the input data for each projection period represents 100 years of TCLV activity, therefore providing more robust track statistics.

The models were grouped based on the frequency of events in the reference period 1981-2010 (Figure 13). This choice is validated by other metrics (e.g. trends in landfall distribution) through the subsequent analysis. However, results will likely vary for a different ensemble selection. There are several studies evaluating the performance of GCMs that can be used to inform model selection (e.g. see Chapter 5 of CSIRO and Bureau of Meteorology, 2015). However, this may not translate to regionally downscaled simulations using those models. The choice of downscaling approach may have a greater influence on performance (Chapter 6 of CSIRO and Bureau of Meteorology, 2015), or on the ability of models to represent TCLV features (Ogata et al., 2016; C. Bruyère, pers. comm.).

GROUP 1	GROUP 2
ACCESS 1.3	ACCESS 1.0
CSIRO Mk 3.6.0	CCSM4
GDFL ESM2M	CNRM CM5
HadGEM2	GFDL CM3
MIROC5	MPI ESM LR
	NorESM1 M

Table 1: Grouping of GCMs for ensemble simulations.

The three key elements that determine the likelihood of extreme winds are:

- frequency of events in the region
- distribution of intensity of those events
- tracks that events take (in this case, we examine only landfall rates along the Queensland coast).

It is important to note the analysis here is focused solely on the changing likelihood of extreme winds. We have not considered the potential changes in TC-related rainfall, which are a major driver of flooding and, when combined with TC winds, water ingress to buildings. There is medium to high confidence of an increase in TC-related precipitation globally of around 14% (Knutson et al., 2020). This will lead to significant impacts to buildings and communities and should be investigated over the Queensland region specifically. Nor have we considered the potential changes in storm surge levels, which is widely projected with high confidence to increase in line with projections of sea level rise (Knutson et al., 2020; McInnes et al., 2015).

3.2 Frequency

The collection of models provides a range of current and future TCLV frequencies. For the reference period (1981-2010), there are two distinct groups of models (Table 1 and Figure 13), with one group around 14 events per year and the second group around 20 events per year.

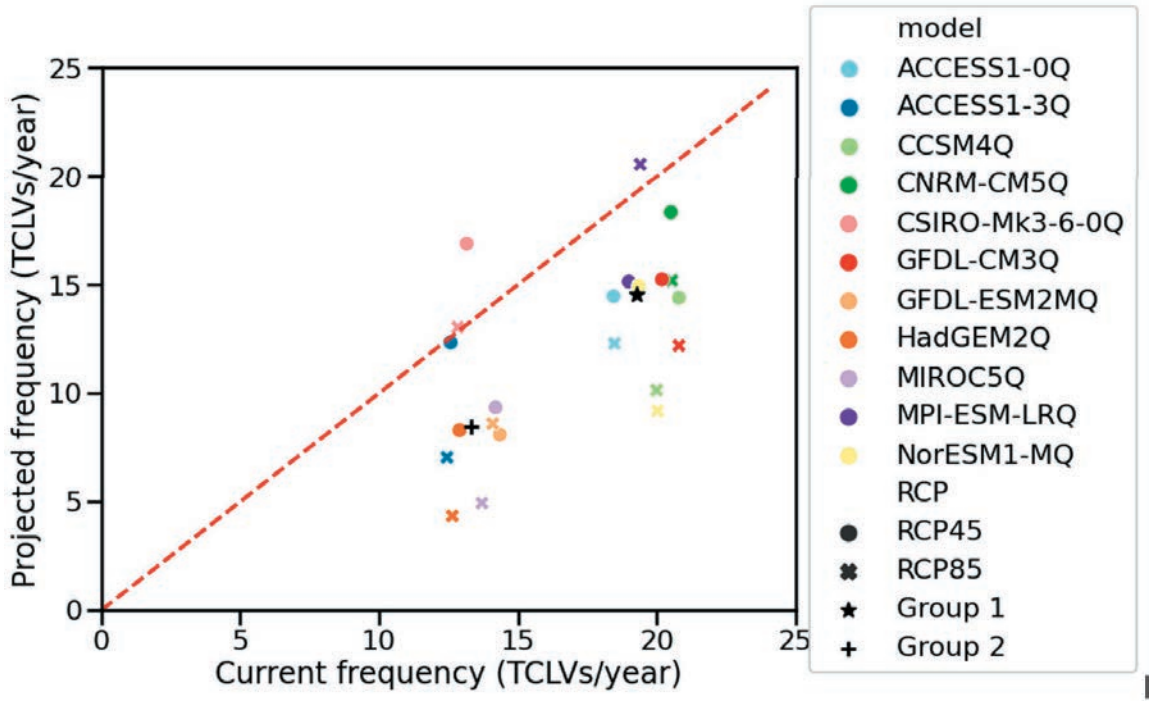

Figure 13: Projected frequency of TCLVs in the suite of 11 RCMs for the future period 2081-2100. Those marked with a filled circle represent the RCP4.5 scenario, 'x' shows the RCP8.5 scenario. The black star and black cross are the ensemble means for automatically classified Group 1 and Group 2 respectively.

3.2.1 Trends in frequency

Generally, there is a declining trend in the frequency of TCLVs detected in the Regional Climate Model (RCM) data. The Group 2 ensemble shows the greatest decline – between 30% and 40% across the two RCPs.

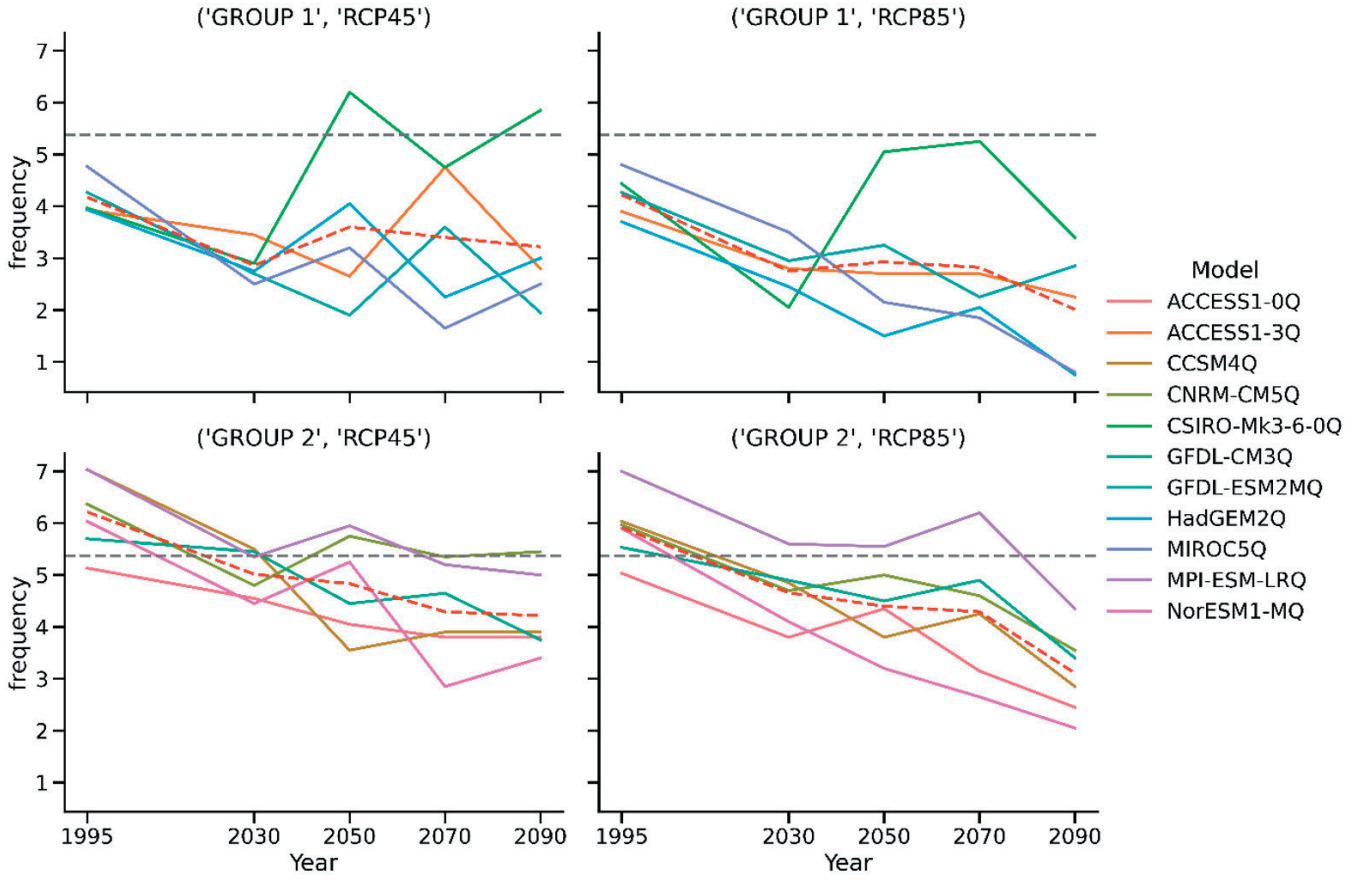

Figure 14: Trends in TCLV frequency for the groups of models (rows) and the emission scenarios (columns). Red dashed line represents the mean of each ensemble, the grey dashed line is the mean historical frequency.

3.3 Intensity

Changes in the distribution of intensity will influence the likelihood of extreme winds. A shift towards more intense TCs would lead to a greater chance of extreme wind speeds. The changes in intensity identified in this analysis are broadly consistent with the projected changes in maximum potential intensity, a thermodynamic index that sets an upper limit on the intensity that can be achieved by a cyclone. Additional information on this analysis will be included in subsequent technical papers.

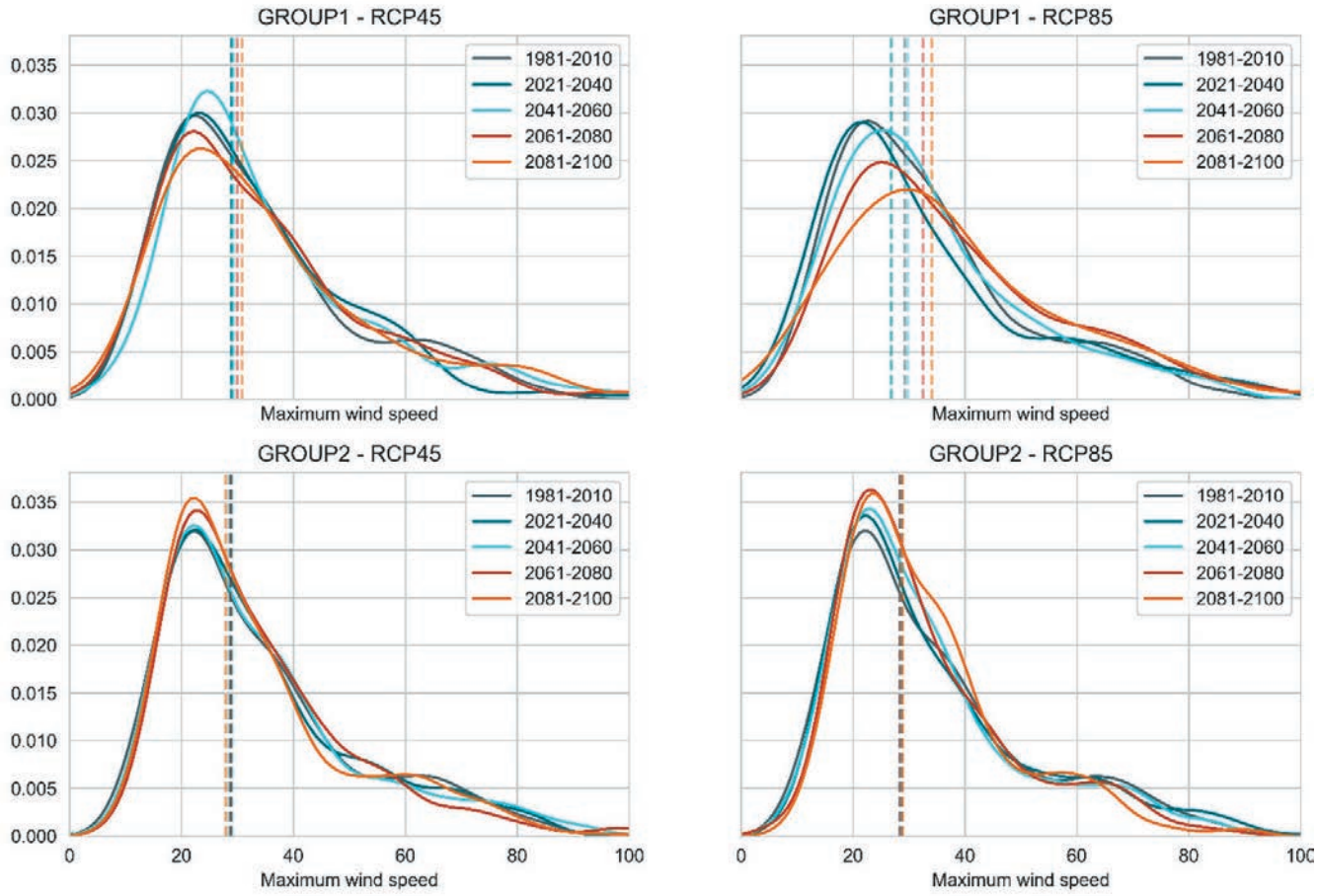

Figure 15: Distribution of maximum intensity (wind speeds, m/s) for combinations of model ensemble groups and emission pathways. The dashed vertical line indicates the median of the distribution for each time period.

Figure 15 presents the probability distribution of maximum intensity (V_{max}) of (scaled) TCLV tracks across the Queensland and Coral Sea region. Group 1, RCP8.5 shows the greatest shift in the distribution of maximum intensity, with a shift in the median of around 10m/s (36km/h). These can be compared to the observed trends in intensity (e.g. Bruyère et al., 2020).

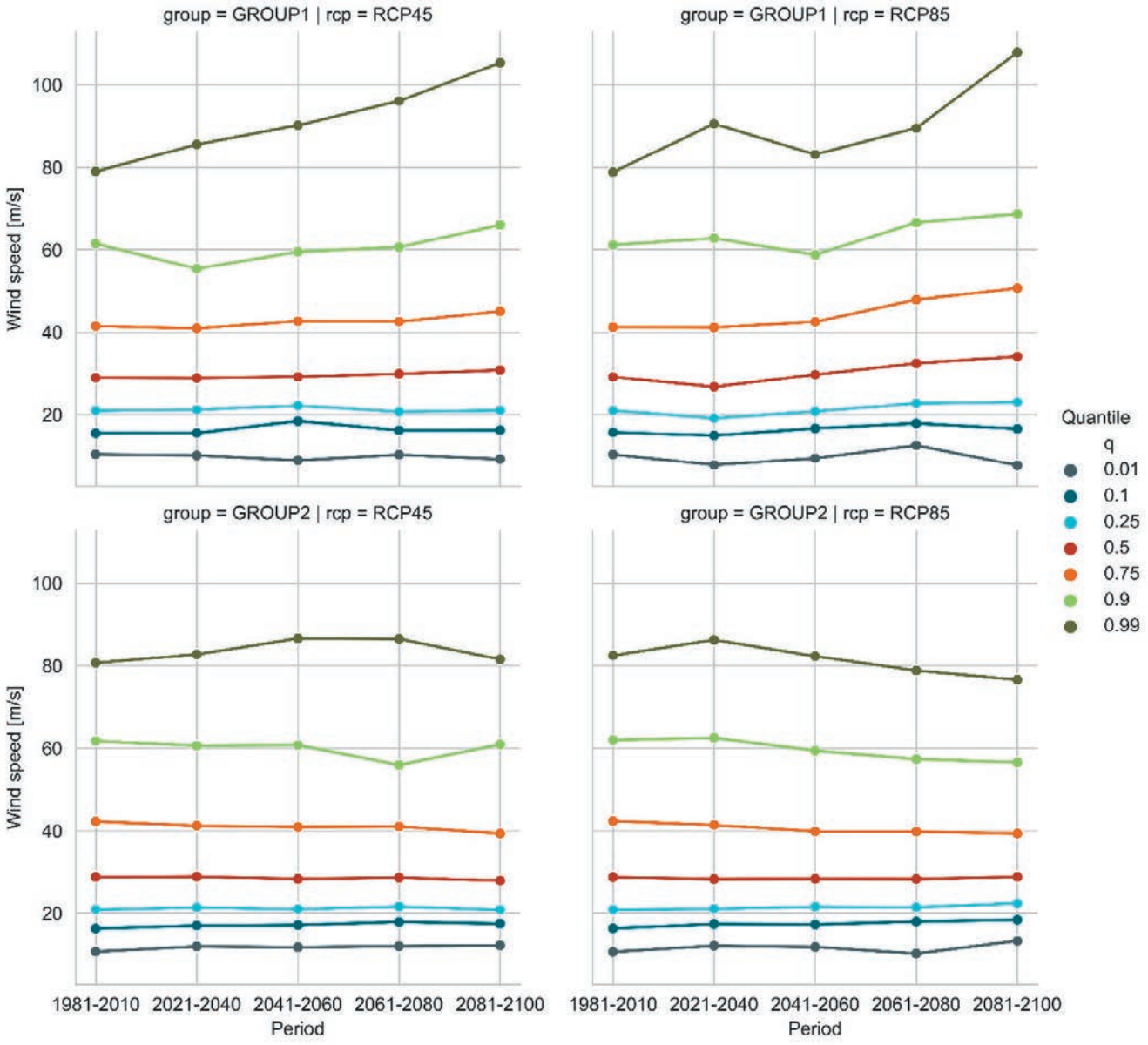

Figure 16: Trends in maximum wind speed quantiles.

Figure 16 shows the trend in quantiles of ^{v}max for (scaled) TCLV data. The quantiles range from 0.01 (the lowest 1% of all ^{v}max) to 0.99 (the highest 1% of all ^{v}max). The different quantiles may display different projected trends.

Both Figure 15 and Figure 16 indicate the Group 1 ensemble are shifting towards a greater proportion of severe TCs in the Queensland region. The Group 2 ensemble displays little change in the median v_{max} and, for the RCP8.5 pathway, a reduction in the intensity of the most extreme events (lower right panel of Figure 16). This should be compared with observed trends in quantiles (Kossin et al., 2013) and changes in intensity (Figure 4 in Knutson et al., 2020).

Consideration should also be given to the latitude of lifetime maximum intensity (λ_{LMI} , Figure 17). Our analysis indicates little significant change in λ_{LMI} for either ensemble or emission pathway. The largest changes based on the TCLV data are for the Group 1 ensemble, RCP8.5 emission pathway, which displays a broadening of the distribution of λ_{LMI} . This is in contrast to the observed trend in λ_{LMI} , which points to a poleward migration of λ_{LMI} both globally and in the South Pacific Basin (Bruyère et al., 2020; Kossin et al., 2014). There is limited confidence in the projections of TC track and occurrence changes (Knutson et al., 2020 and references therein), so our results are considered another view of the possible future behaviour.

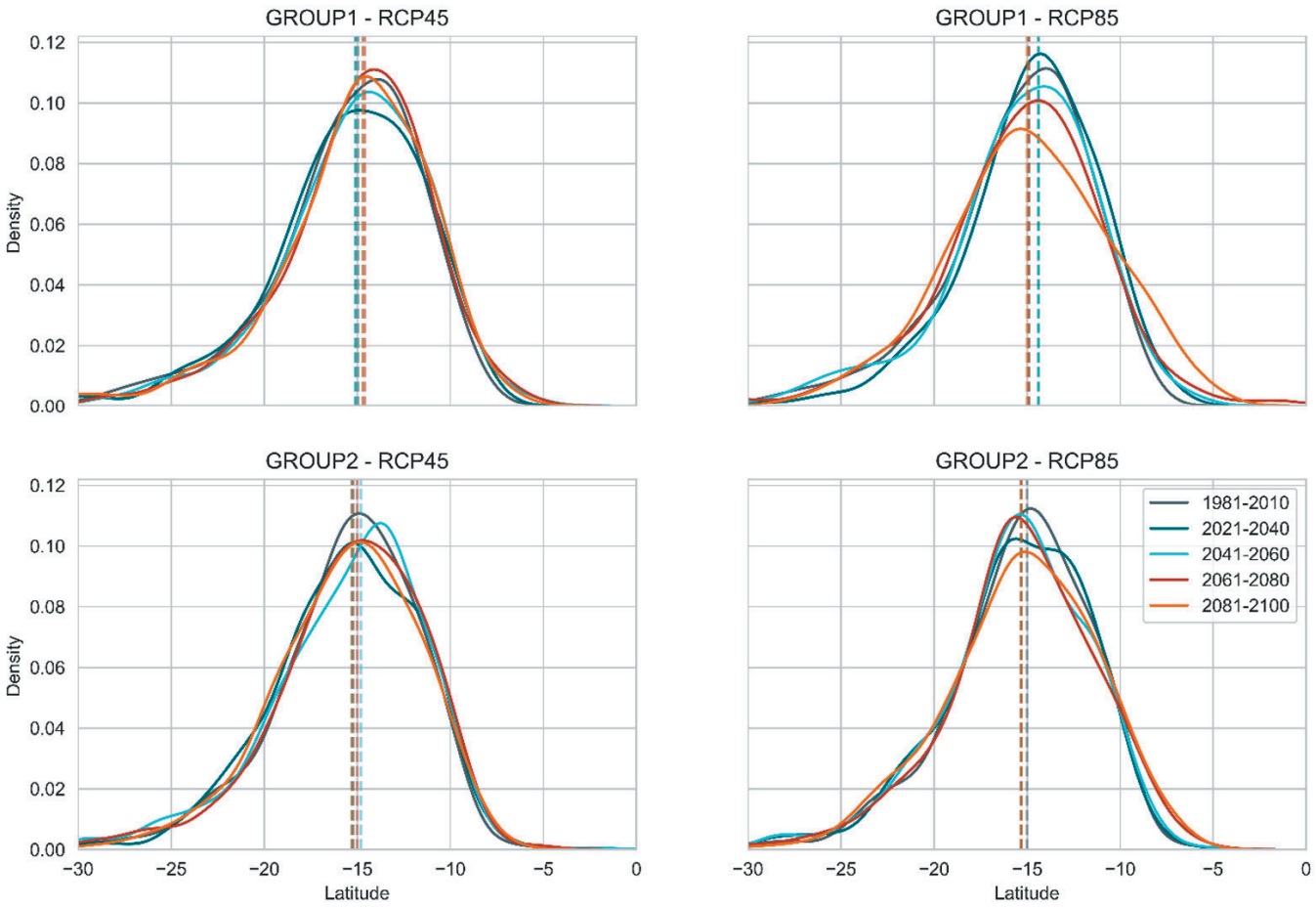

Figure 17: Latitude of lifetime maximum intensity for the ensembles and RCP pathways. The dashed vertical line indicates the median λ_{LMI} for each time period.

3.4 Landfall

Landfall is a useful indicator, as risks from TC winds are realised when TCs impact communities. Landfall is widely used as a predictor of how 'active' (or otherwise) a hurricane season is likely to be in the Atlantic and elsewhere (Hall and Jewson, 2008; Hall and Yonekura, 2013; Holland, 2007; Kriesche et al., 2014; Weinkle et al., 2012). We determine landfall rates by examining the frequency of TCs crossing a series of 200km wide 'gates' placed along the coastline set 50km off the coast (refer Figure 11). The intensity at landfall is recorded so we can separate severe and non-severe TCs.

Changes in landfall rates for TCs along the Queensland coast are indicative of the changes in track behaviour arising due to climate change. For example, the poleward (southwards) migration of TCs due to the expanding Hadley circulation (Bruyère et al., 2020; Kossin et al., 2014) would be reflected in an increased rate of landfalling TCs further south along the coastline.

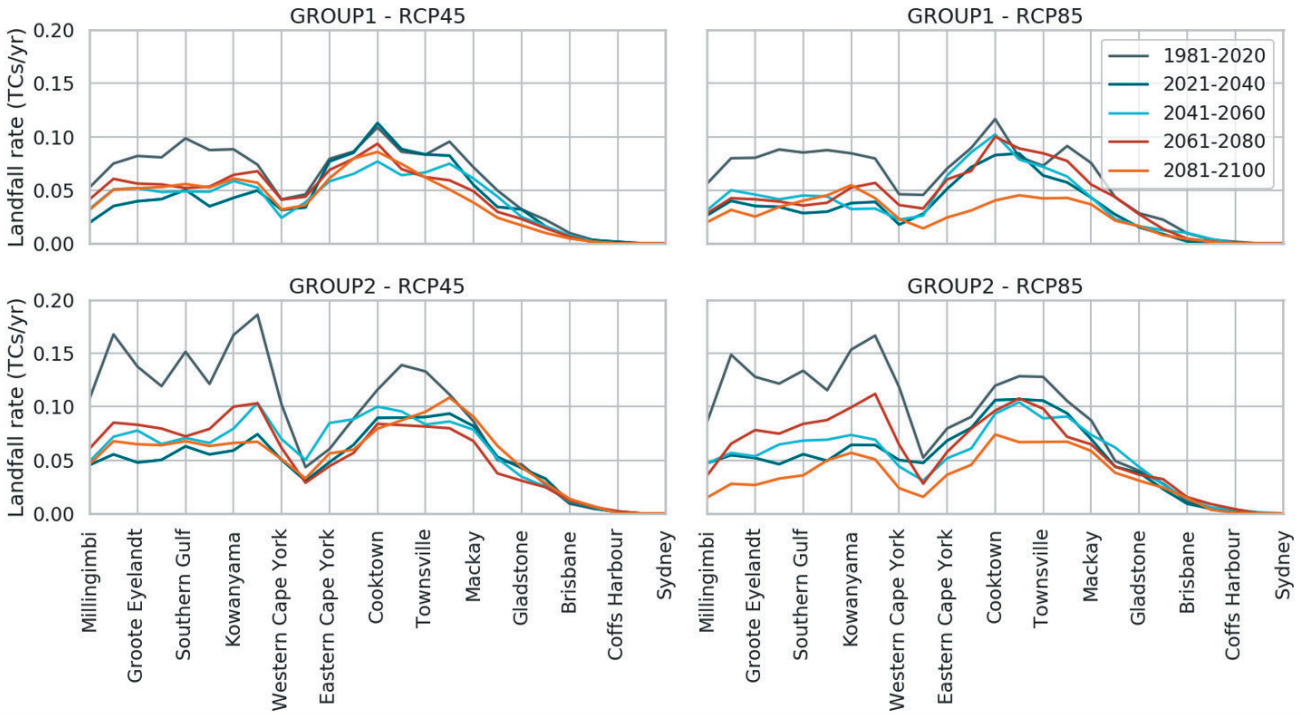

Figure 18: TC landfall rates for Queensland coastline for reference and future time periods. These landfall rates are based on 10,000 simulated years of TC activity for each time period.

Landfall rates along the Queensland coast are sensitive to the overall frequency of events in each ensemble – the Group 2 ensemble has a higher mean frequency of TCs in the reference and future climate simulations. There are also very few landfalls recorded in South East Queensland, so relative changes are likely to be large, but not necessarily statistically significant.

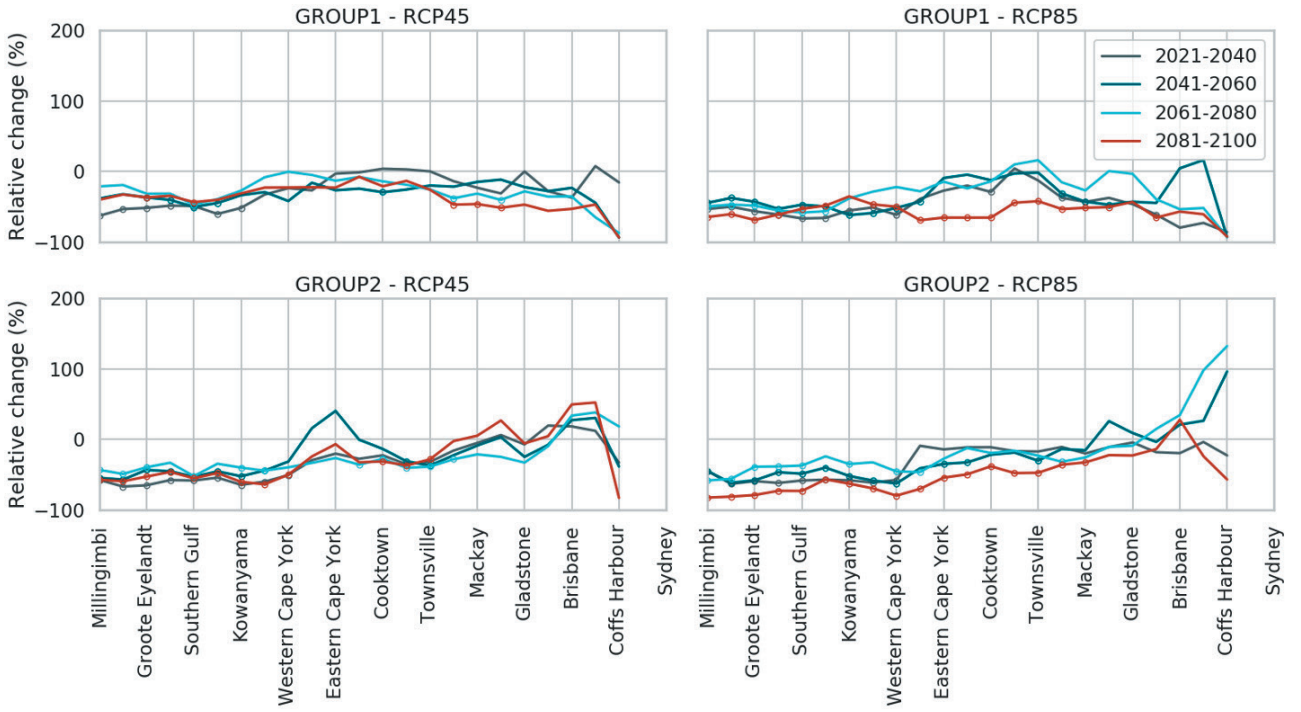

Figure 19: Relative change in landfall rates for future time periods compared to the reference period (1981-2010). Statistically significant changes ($p < 0.05$) are marked with an open circle.

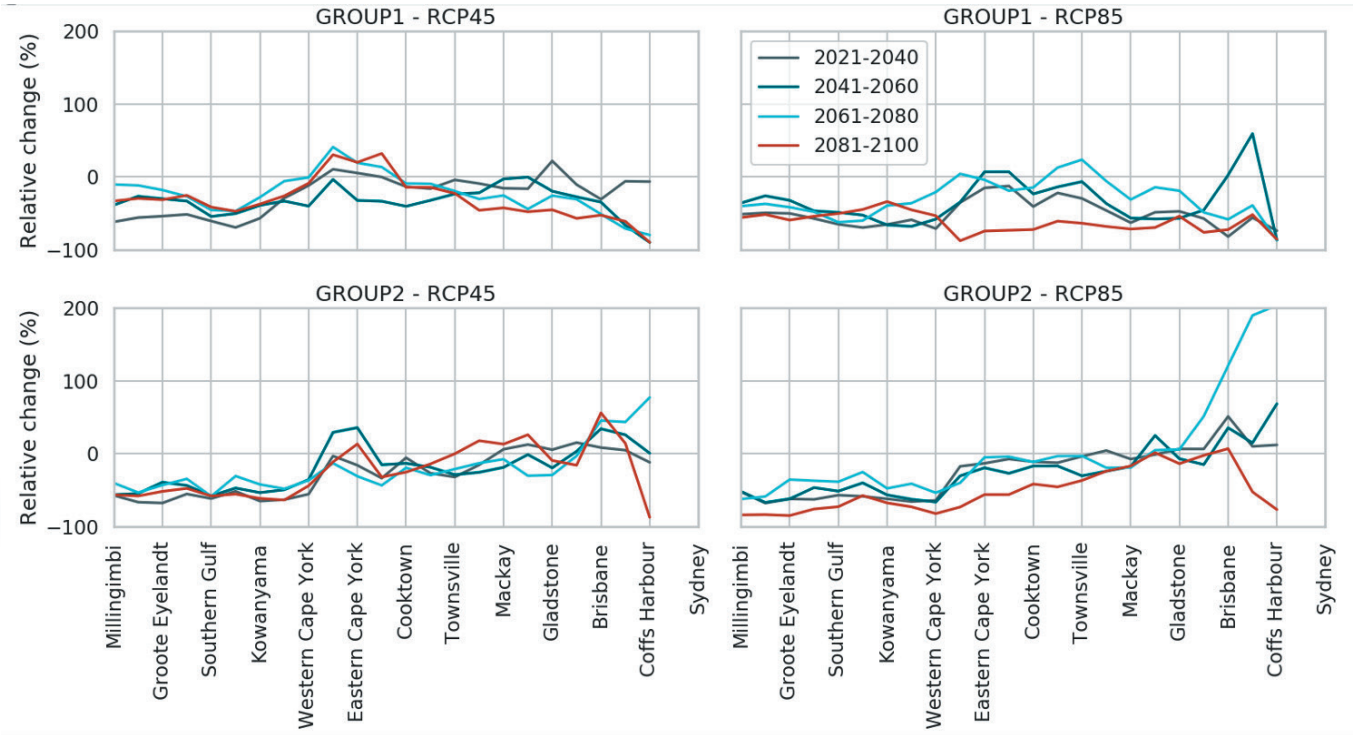

Figure 20: Relative change in landfall rates for severe TCs (Category 3-5) for future time periods, compared to the reference period (1981-2010). None of the changes are considered statistically significant.

The Group 1 ensemble indicates a decrease in the rate of landfall right along the coast, with a greater decrease in the RCP8.5 scenario. In the Gulf of Carpentaria (Milingimbi – Western Cape York) there is around a 50% reduction in landfall rate across all models. The Group 2 ensemble indicates an increase in the rate of landfall in central and southern Queensland (about Mackay southwards). Note the rate of landfall in the reference period in South East Queensland is very low, and the changes are not all statistically significant.

In summary, the analysis indicates the following key points:

- The declining frequency and relatively small shift in the distribution of TC intensity suggests that likelihood of extreme wind speeds (with reference to annual exceedance probability) will be reduced into the future.
- The Group 1 ensemble does show the most extreme events becoming more intense (Figure 16), however, the reduced frequency will largely offset this when viewed in terms of annual exceedance probability.
- There may be some regional variations around this – for example the Group 2 ensemble indicates a relative increase in TC landfall over the southern half of the Queensland coast (not statistically significant). In this case, the increasing rate of landfall in southern Queensland would warrant further investigation around emergency management provisions and resources, as well as longer-term mitigation options to reduce potential impacts from more frequent TCs.

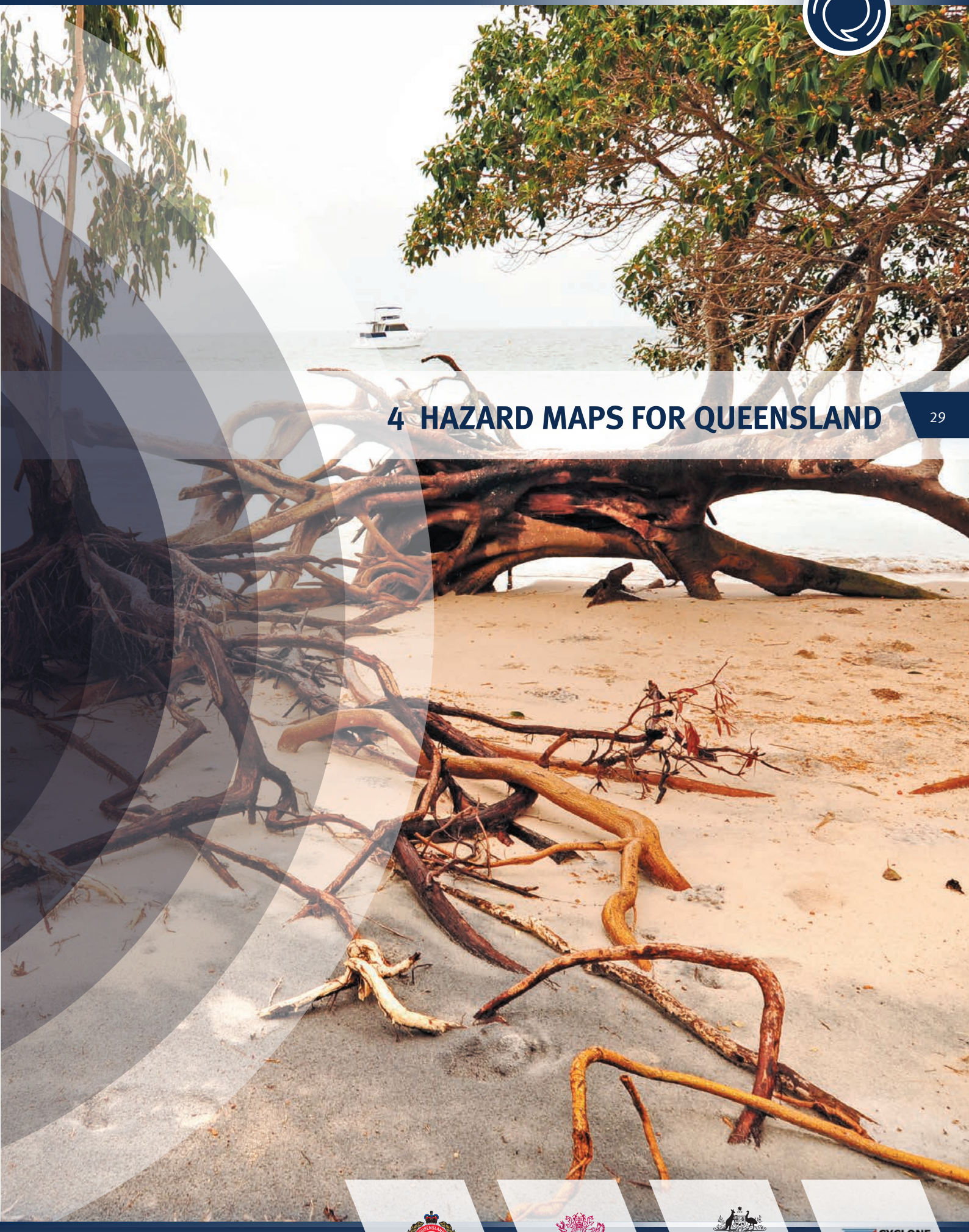

4 HAZARD MAPS FOR QUEENSLAND

Queensland Government
Australian Government
Geoscience Australia
CYCLONE TESTING STATION

4 Hazard maps for Queensland

The modelled hazard maps integrate the frequency of events with the intensity distribution to provide a spatial representation of the likelihood of extreme winds. We use the average recurrence interval (ARI) to describe the likelihood. The larger the ARI, the lower the likelihood of that wind speed being exceeded – that is, a 500-year ARI is less frequent than a 100-year ARI.

The likelihood of exceeding a given AEP in a period of time (e.g. 50 years) is set out in Appendix B.

We present the 1% AEP and 0.2% AEP wind speed maps in Figure 21 to Figure 30, which have a likelihood of approximately 40% and 10% respectively over a 50-year period.

4.1 1% annual exceedance probability wind speeds

The 1% AEP wind speed corresponds to approximately a 10% probability of occurrence in 50 years (refer Appendix B).

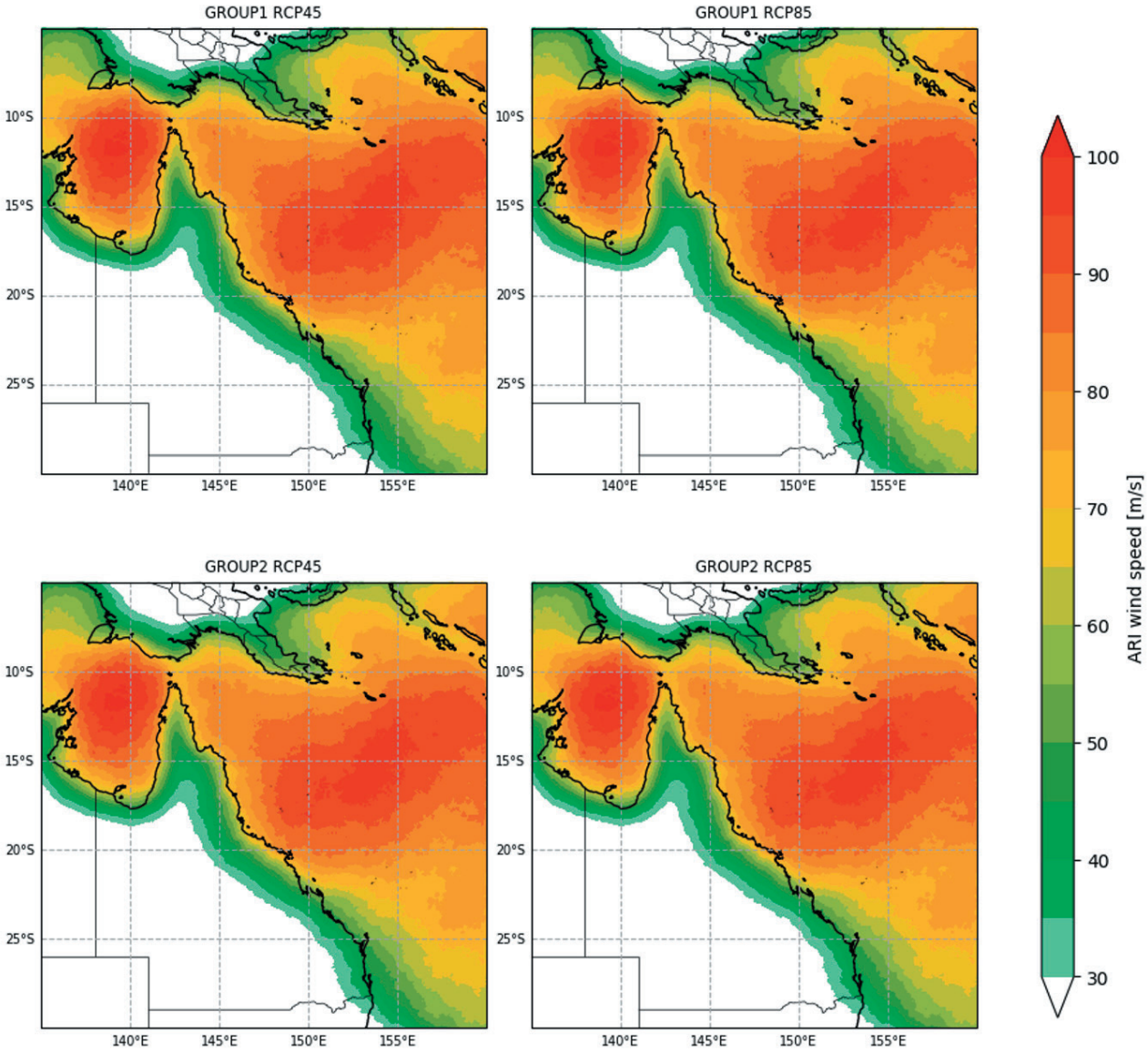

Figure 21: 1% AEP wind speed for Queensland, for the period 1981-2020.

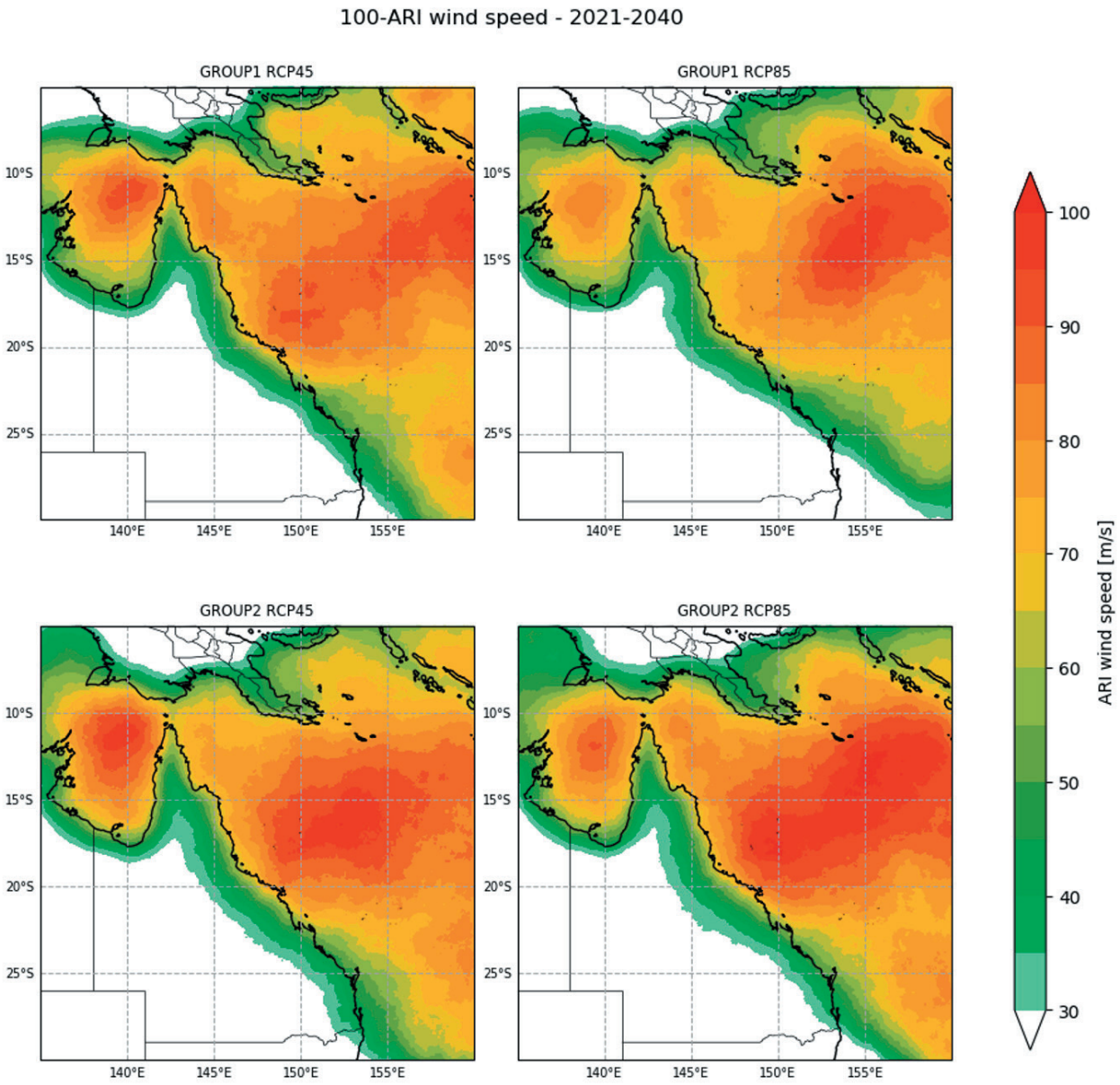

Figure 22: 1% AEP wind speed for Queensland, for the period 2021-2040.

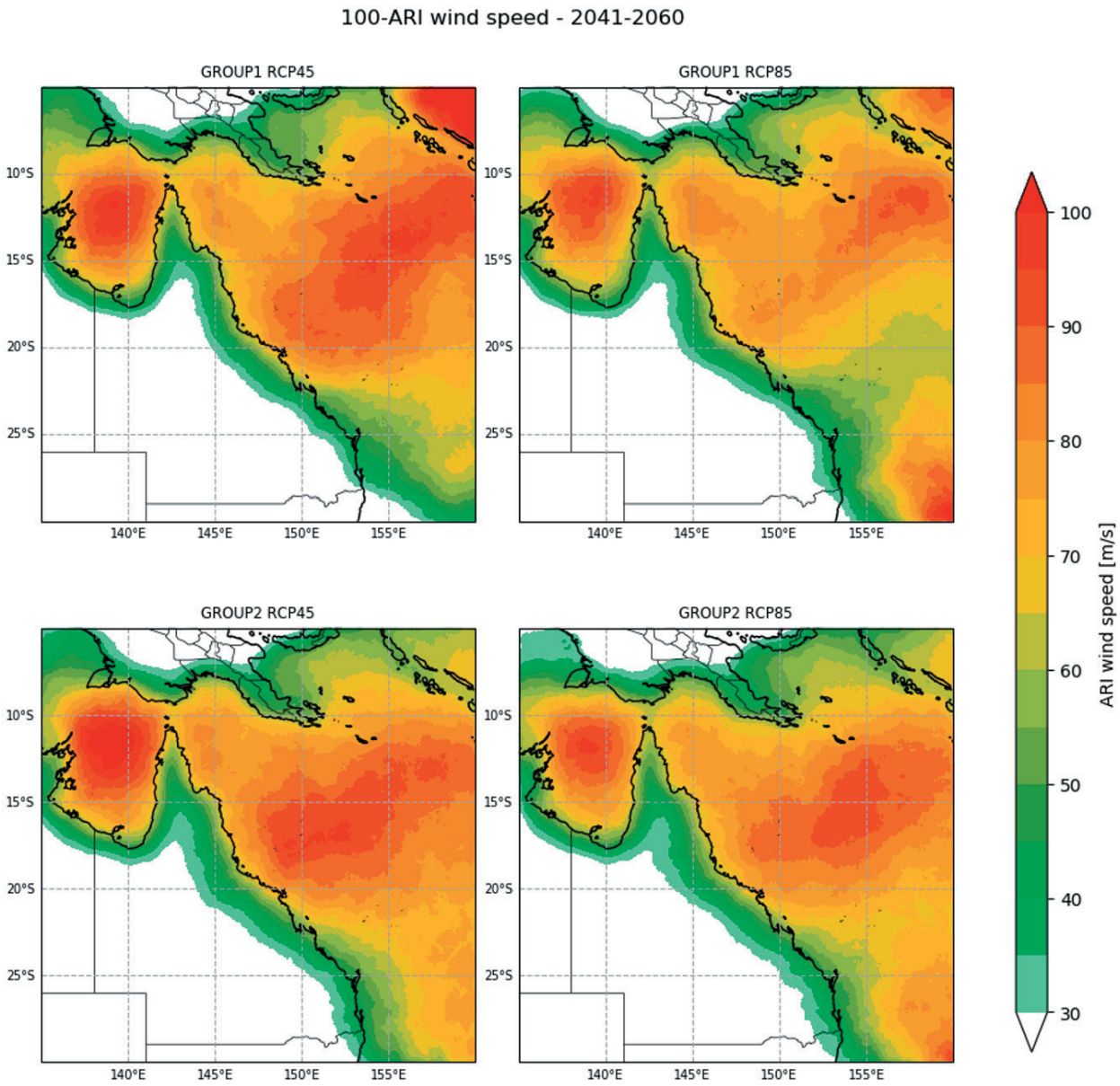

Figure 23: 1% AEP wind speed for Queensland, for the period 2041-2060.

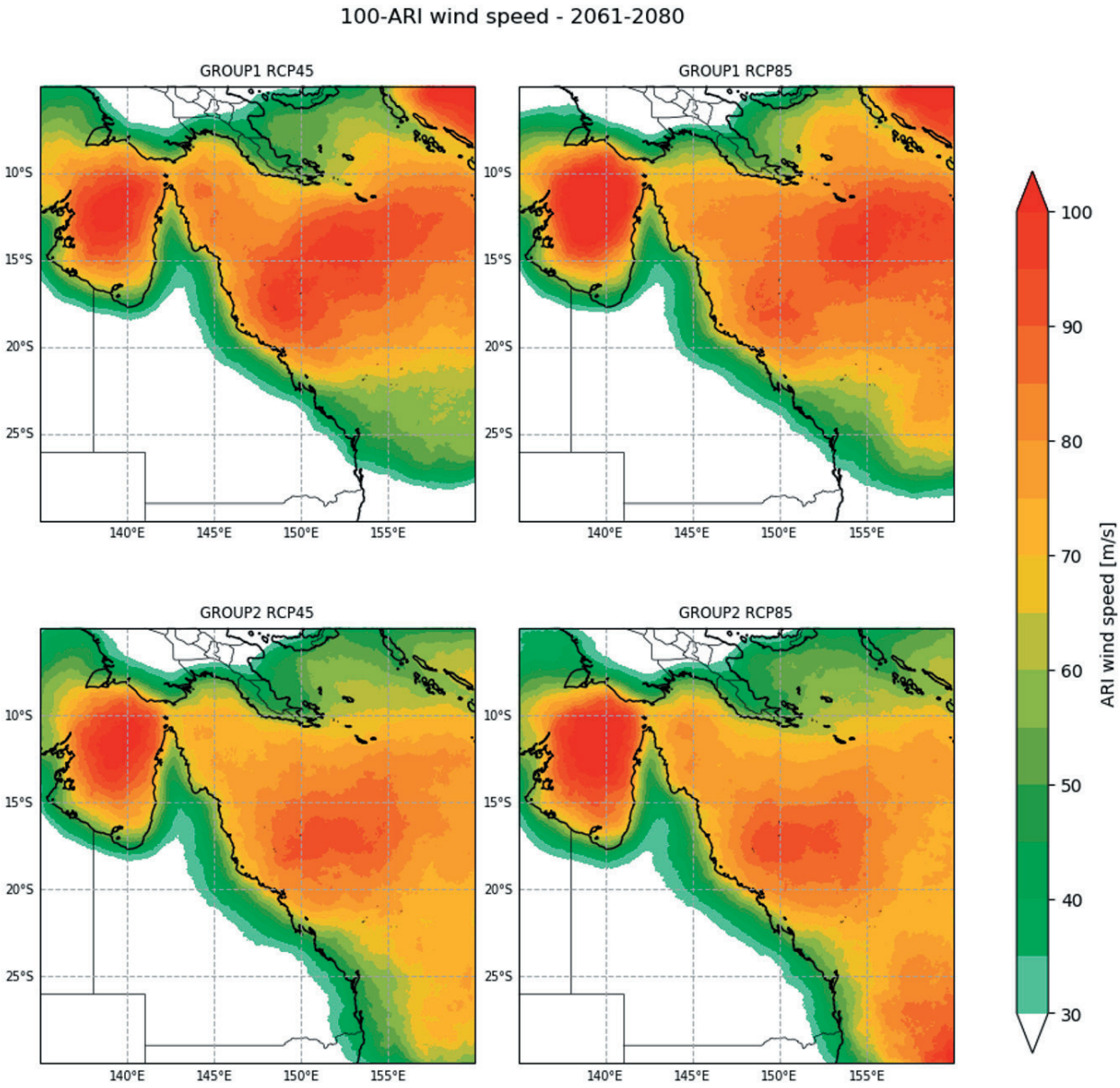

Figure 24: 1% AEP wind speed for Queensland, for the period 2061-2080.

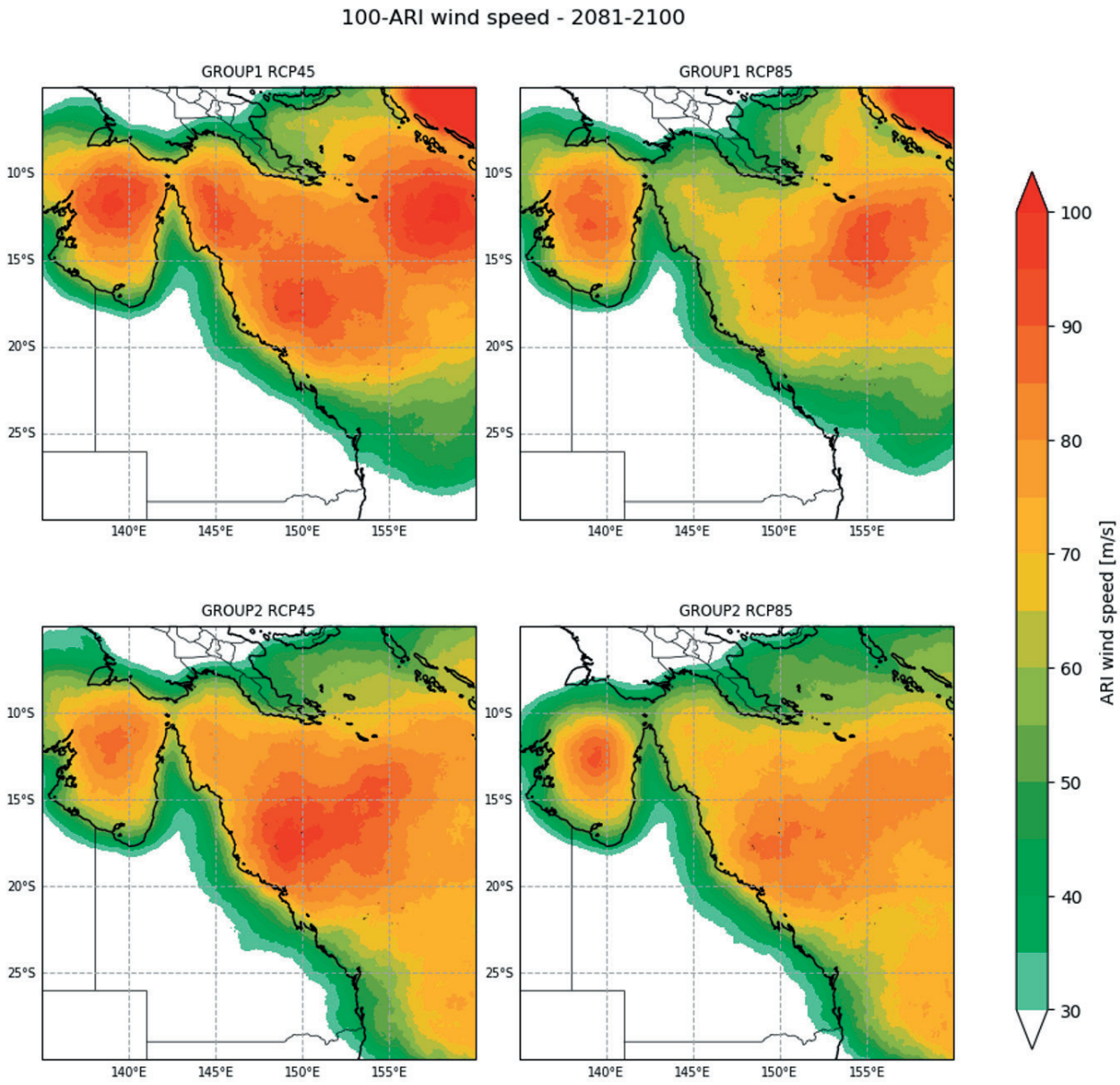

Figure 25: 1% AEP wind speed for Queensland, for the period 2081-2100.

4.2 0.2% annual exceedance probability wind speed maps

This section presents 0.2% AEP (500-year ARI) wind speed maps for each time period from 2021-2040 through to 2081-2100. The 0.2% AEP wind speed corresponds to approximately a 10% probability of occurrence in 50 years (refer Appendix B). This also corresponds to the regional design wind speed for residential houses.

Progressing through the time periods, there is a decline in the wind speeds through the central Queensland coast but little change at the southern edge of the region. Some interdecadal variability can be seen but is more clearly displayed in the change maps shown in Figure 26 to Figure 30.

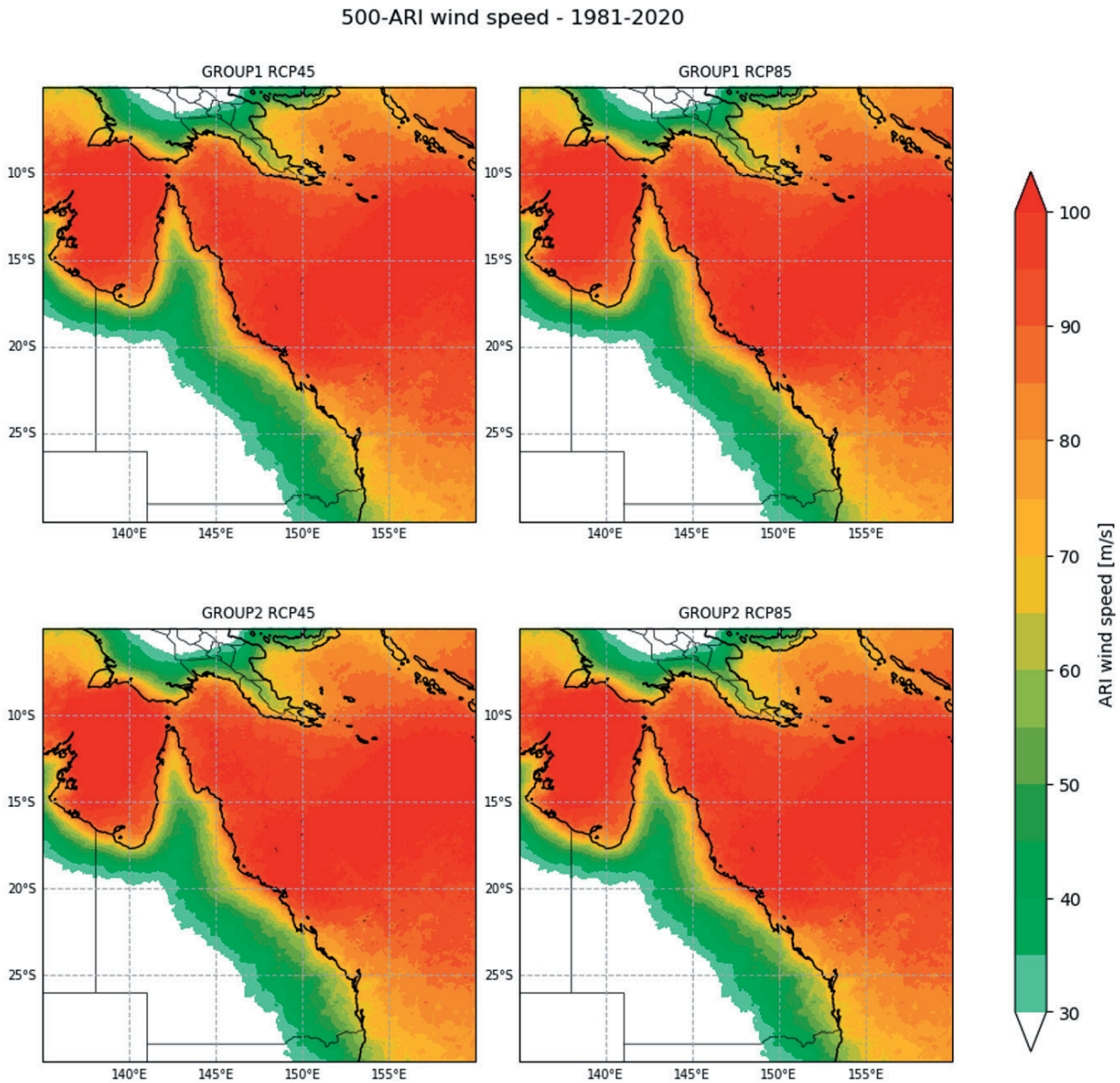

Figure 26: 0.2% AEP wind speed for the period 1981-2020, based on the RCM-derived TC climate.

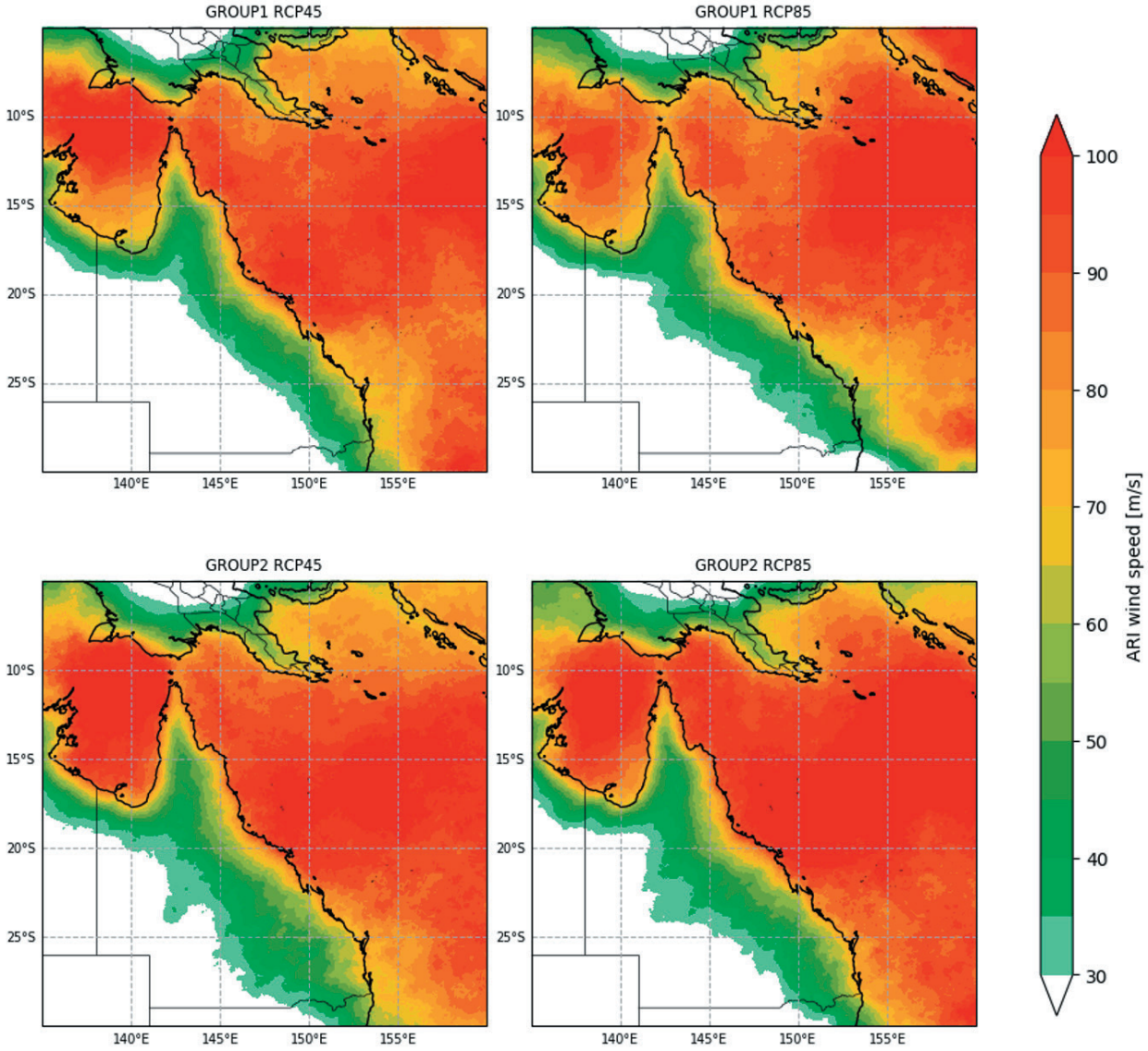

Figure 27: 0.2% AEP wind speed for the period 2021-2040, based on the RCM-derived TC climate.

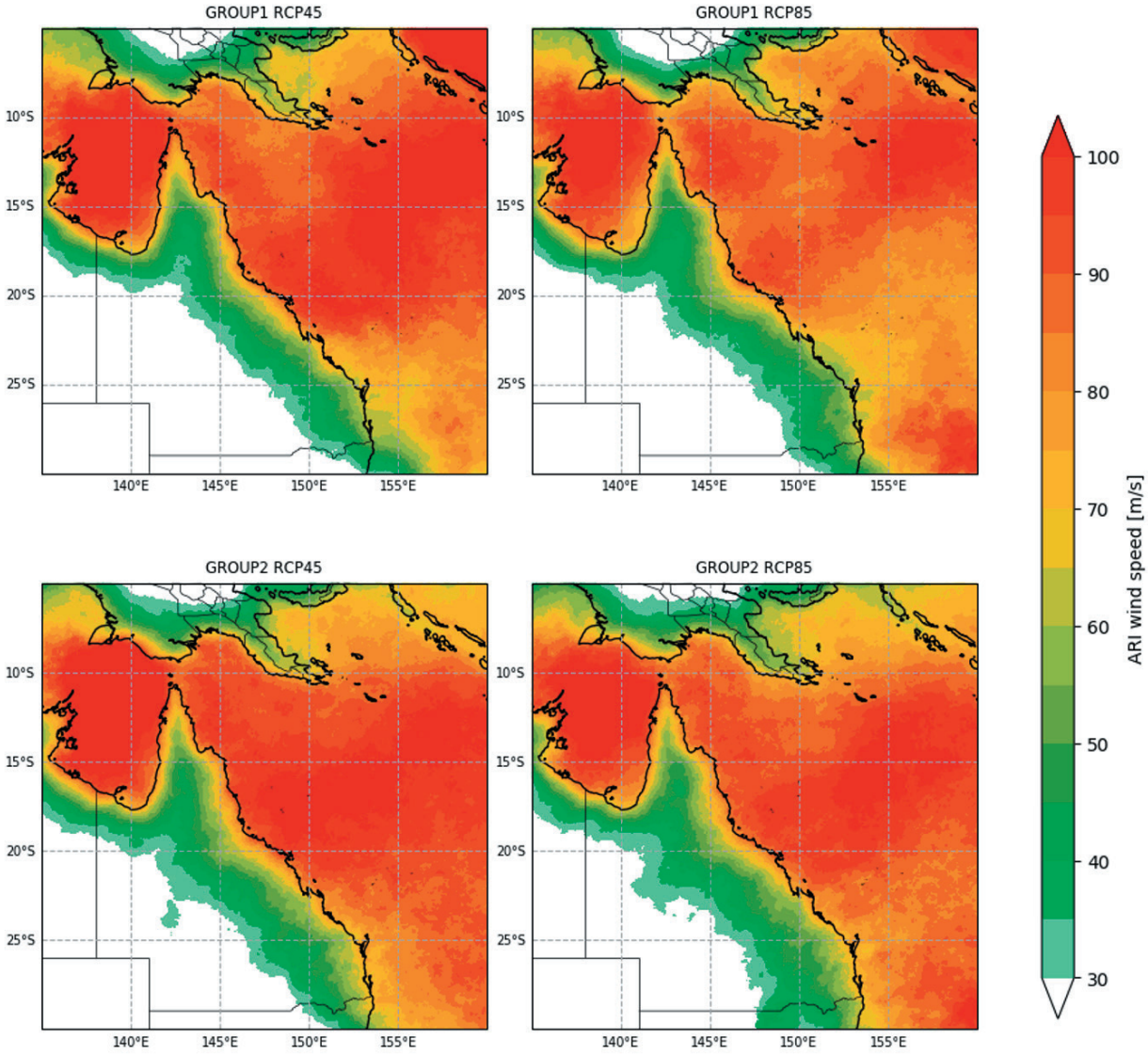

Figure 28: 0.2% AEP wind speed for the period 2041-2060, based on the RCM-derived TC climate.

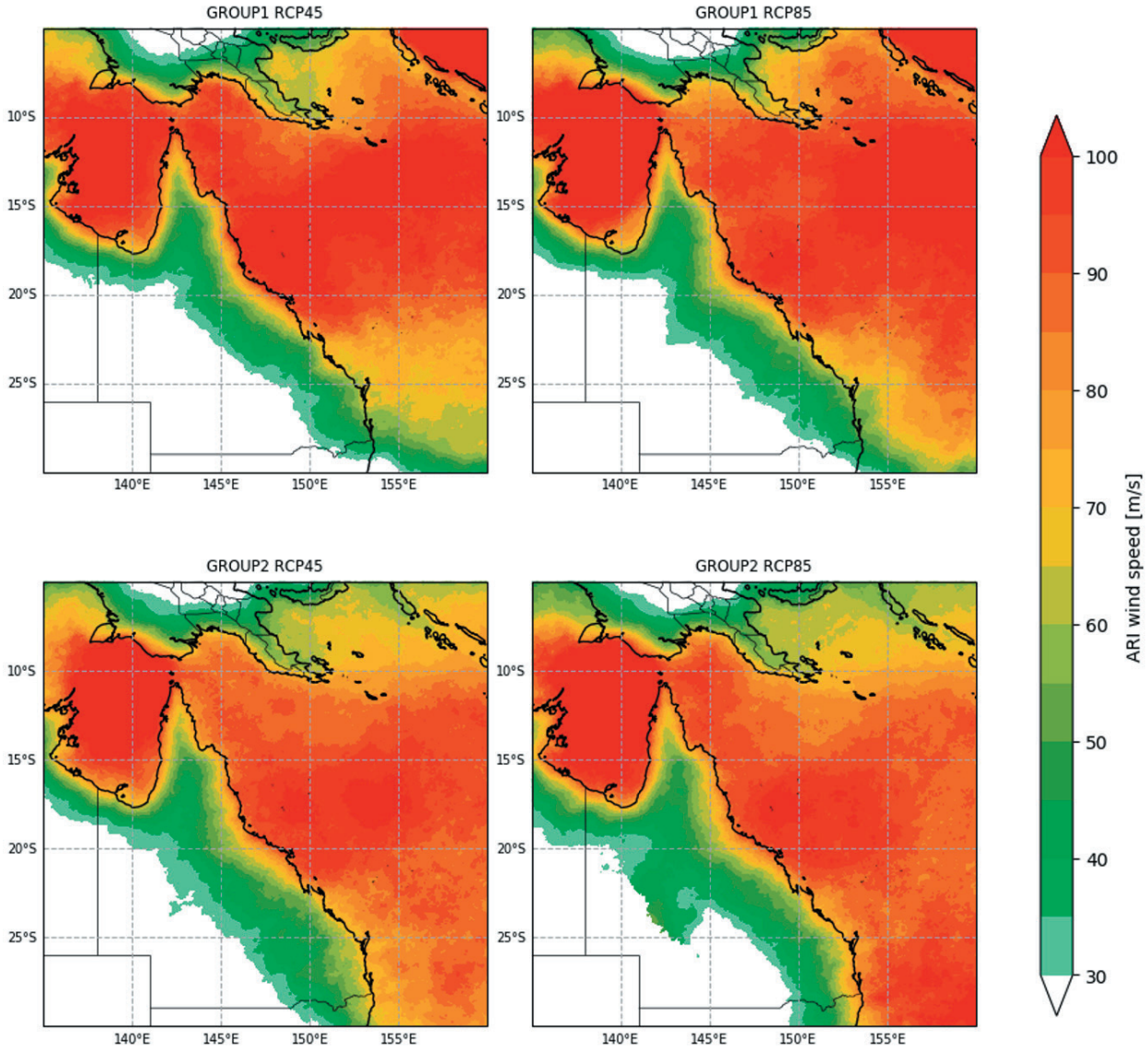

Figure 29: 0.2% AEP wind speed for the period 2061-2080, based on the RCM-derived TC climate.

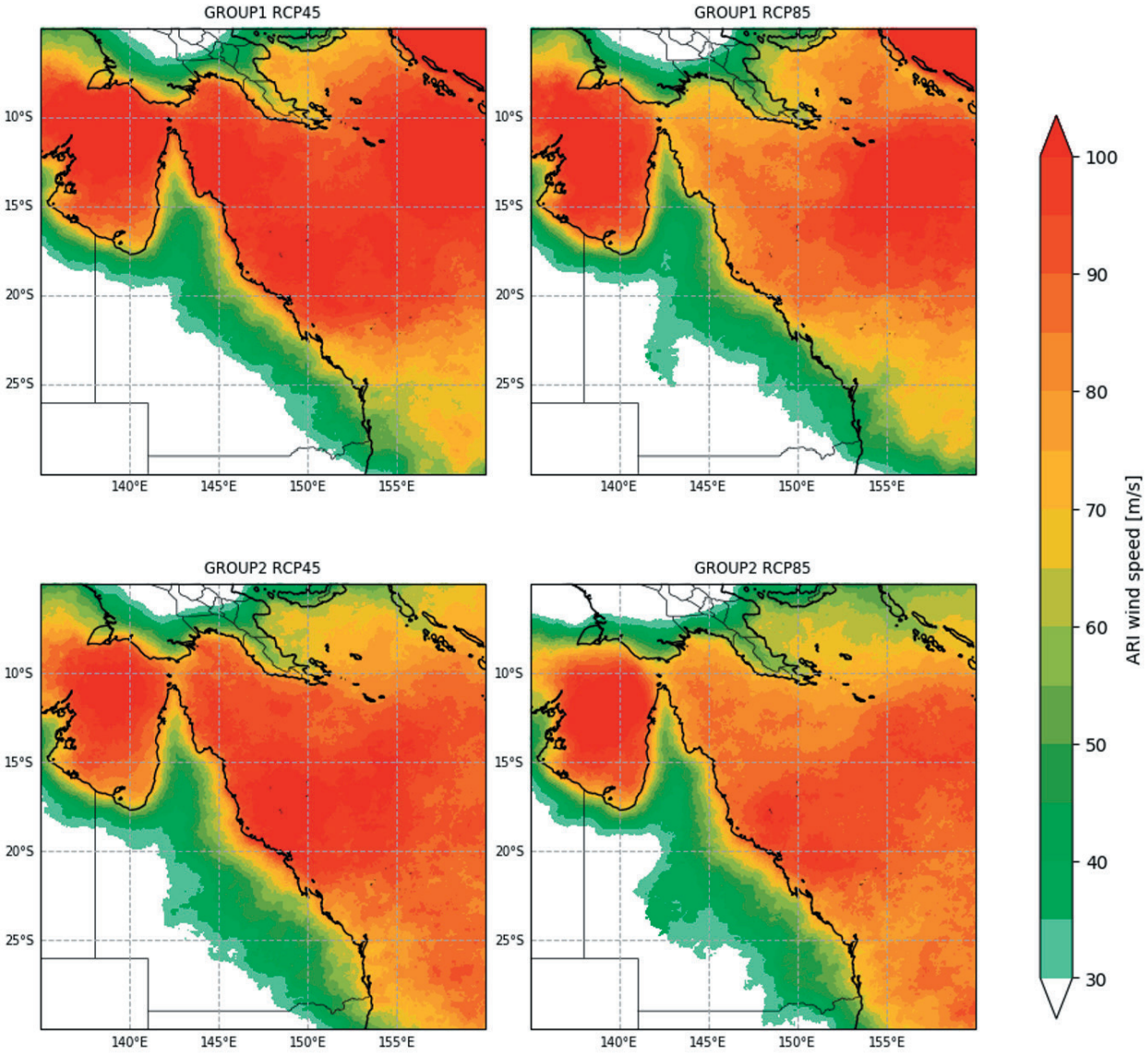

Figure 30: 0.2% AEP wind speed for the period 2081-2100, based on the RCM-derived TC climate.

4.3 Changes in hazard

We present the absolute change in modelled wind hazard for the 0.2% AEP (500-year ARI) wind speeds for each 20-year time period in Figure 31 to Figure 34.

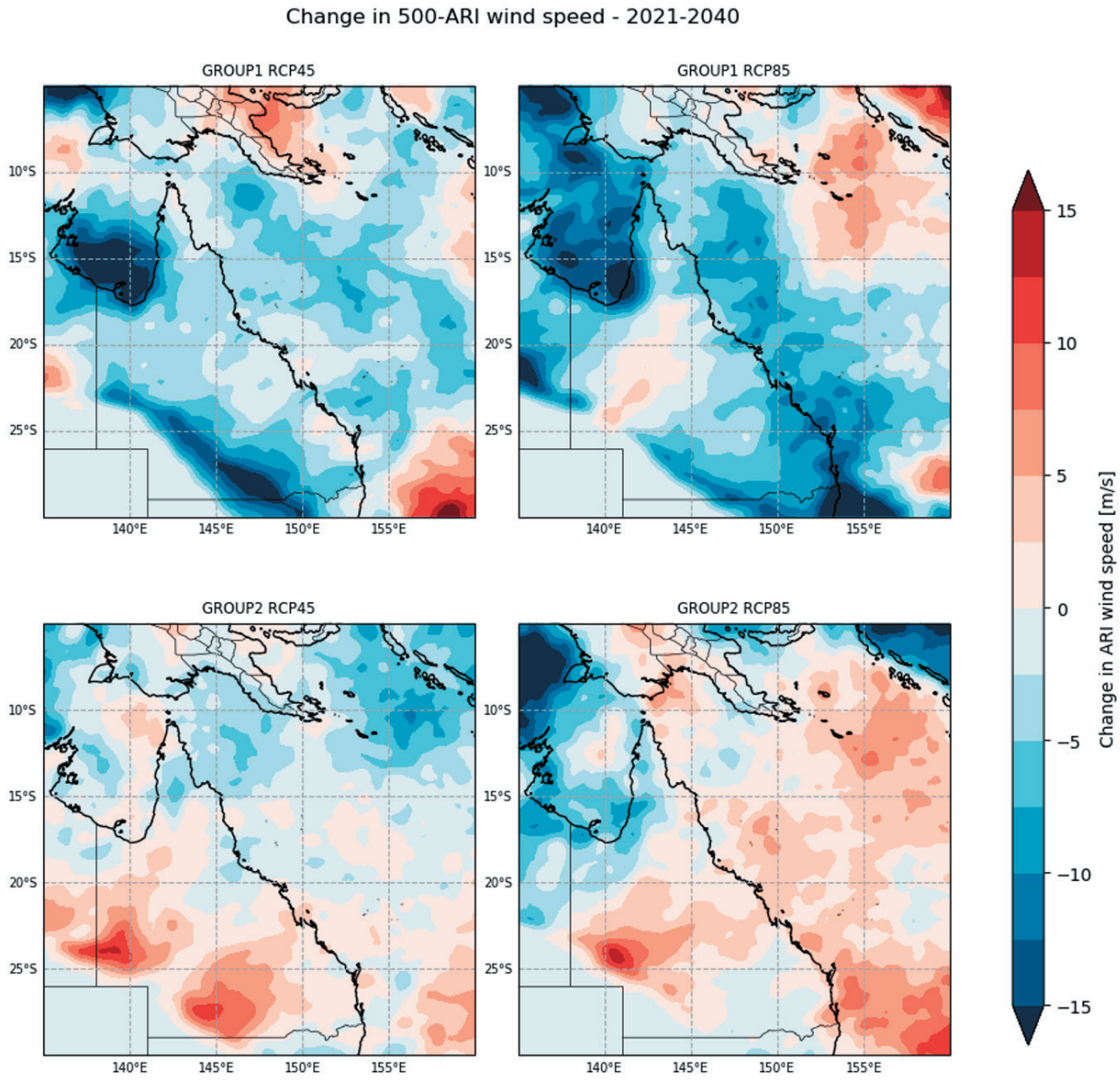

Figure 31: Change in 0.2% AEP wind speed for Queensland for the period 2021-2040.

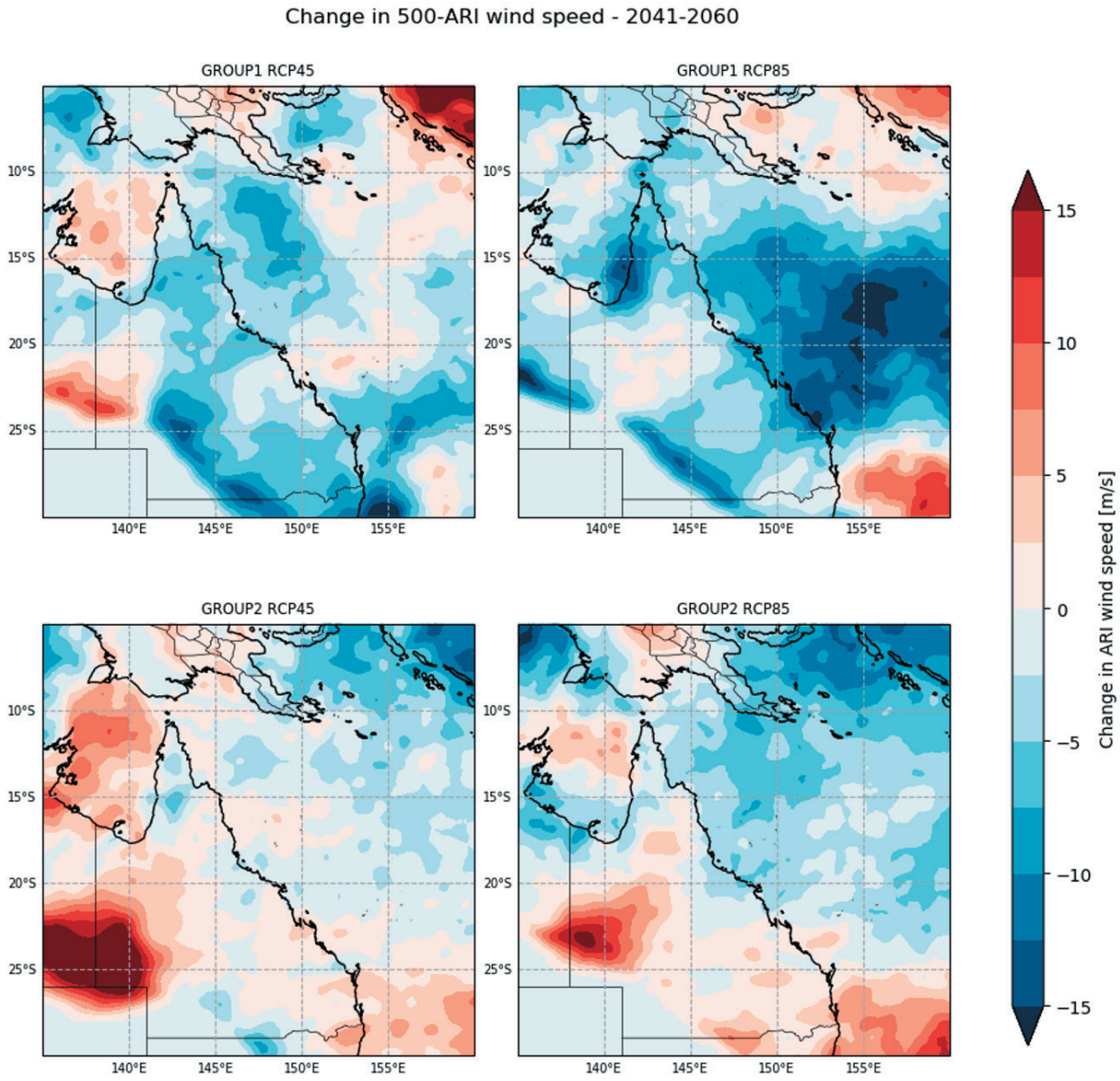

Figure 32: Change in 0.2% AEP wind speed for Queensland for the period 2041-2060.

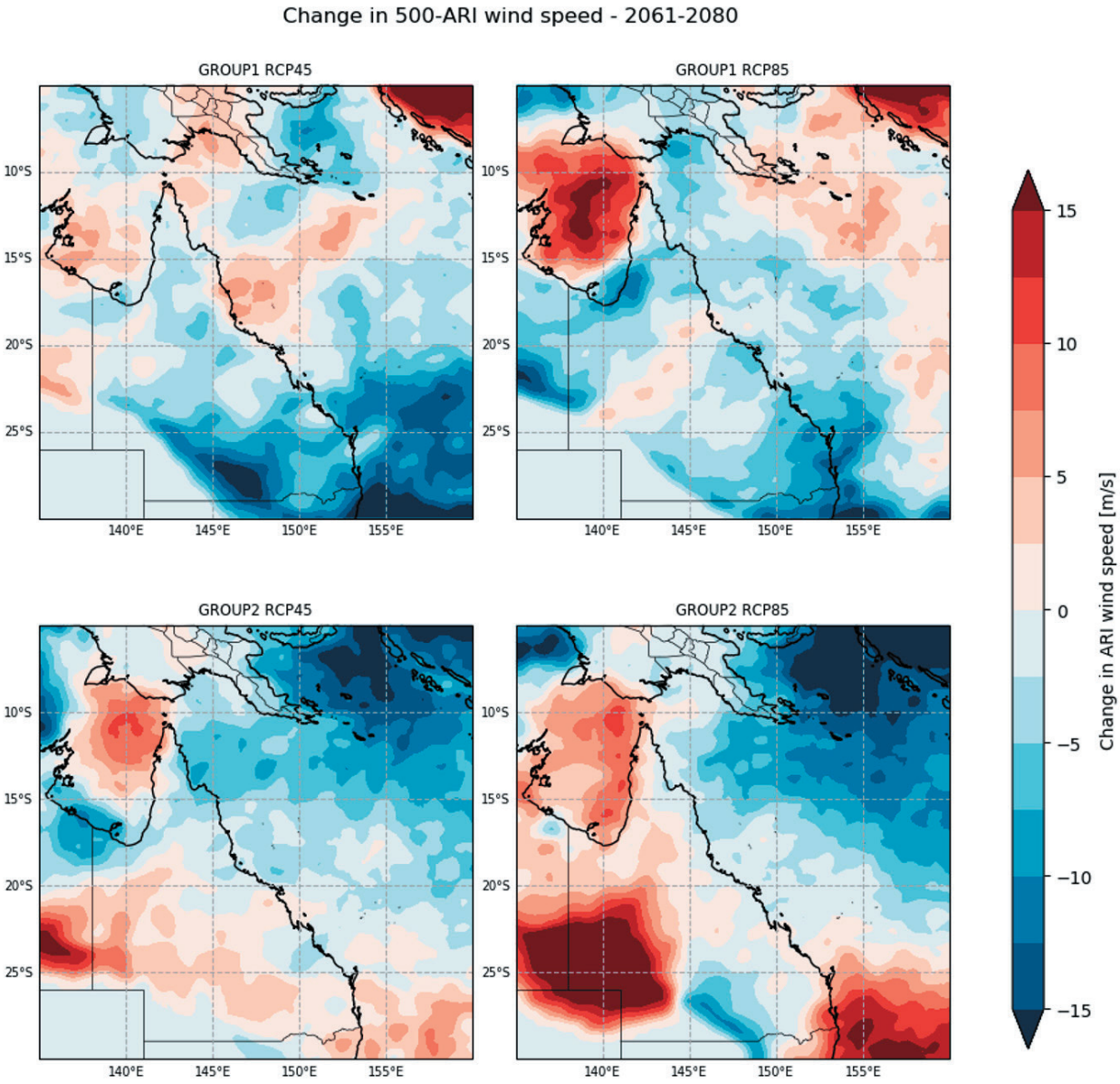

Figure 33: Change in 0.2% AEP wind speed for Queensland for the period 2061-2080.

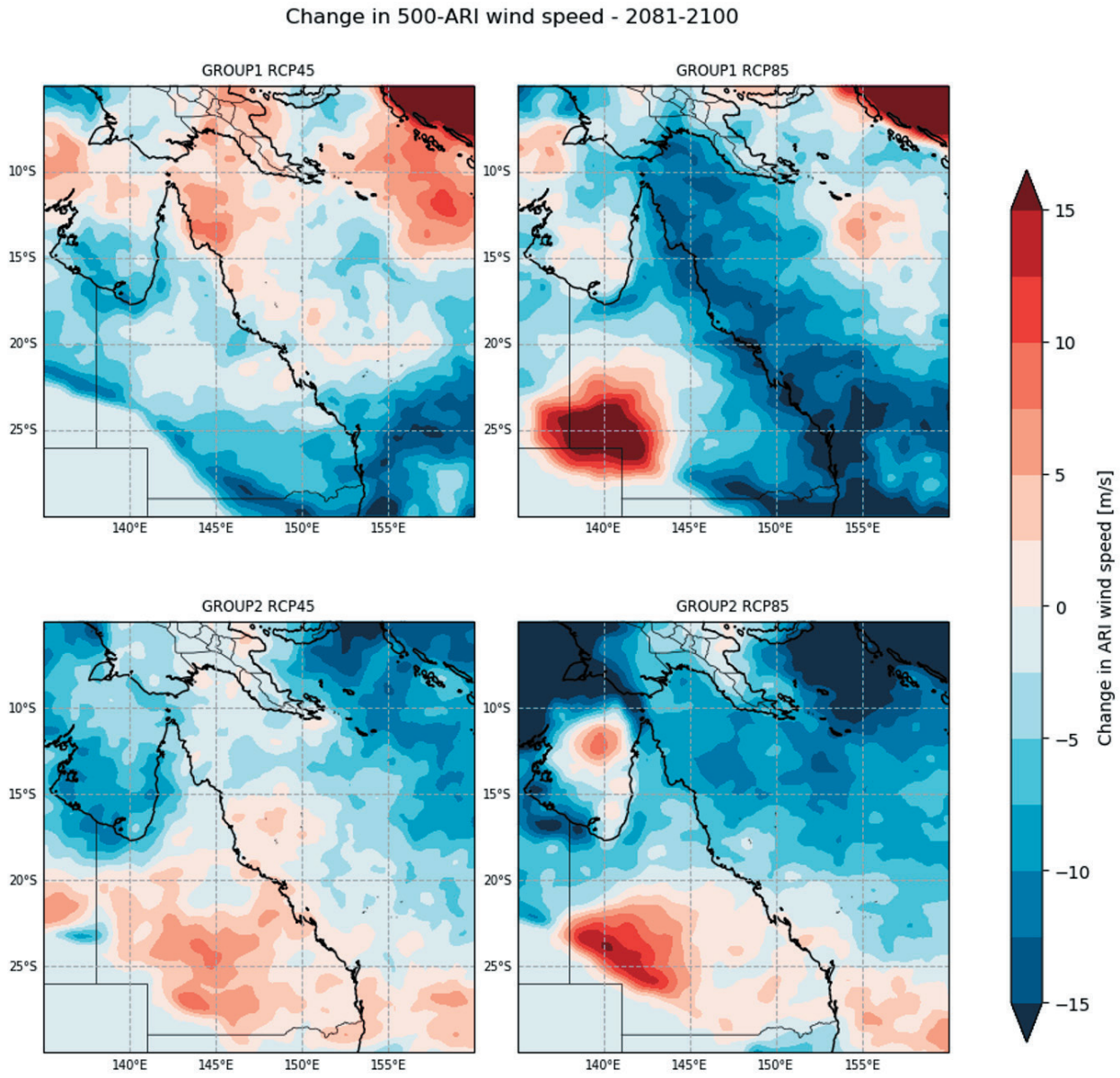

Figure 34: Change in 0.2% AEP wind speed for Queensland for the period 2081-2100.

The Group 1 ensemble shows a consistent decline in 500-year ARI hazard through to end century time frames, with the RCP8.5 scenario indicating reductions of greater than 15m/s (54km/h) along the entire Queensland coast. Conversely, the Group 2 ensemble indicates a slight decrease in hazard north of the Whitsundays (excluding the Gulf of Carpentaria), and a slight increase in hazard (<5m/s) south of 20°S. Note that large changes in hazard through inland Queensland are unlikely to be statistically robust, owing to the low occurrence of TCs in that region.

Given the interdecadal variations (i.e. from one time period to the next), there may only be low confidence in the projected wind hazard changes towards the end of the century. A shortcoming of the approach of this study is the limited record for each 20-year period used as input to the hazard simulations. This can make the hazard assessment overly sensitive to the fluctuations of the TC activity between time periods. While we have attempted to address this by merging multiple RCMs into two ensembles, there remains some scope to further bolster the quality and quantity of data to be used as input into this analysis by using a broader suite of downscaled climate models, or by using multiple realisations from each of those RCMs.

5 PROJECTIONS OF HAZARD PROFILES FOR COMMUNITIES

5 Projections of hazard profiles for communities

Hazard profiles present the likelihood (probability) of exceeding wind speed levels in any given year. Referring to Figure 35 to Figure 40, the horizontal axis is the wind speed levels and the vertical axis is the probability of exceeding that wind speed in any year. Higher wind speeds have a lower probability, so the curve slopes downward from upper left to lower right.

A decrease in the intensity of wind speeds will shift the curve to the left, while an increase in the intensity of winds will shift it to the right. In the case of a change in the distribution of intensity, an increase in the proportion of intense TCs will act to flatten the curve, while a shift towards a greater proportion of weak storms will make the curve steeper. A decrease in the annual frequency of TCs will shift the curve directly downwards (lower overall probability) and an increase in frequency will shift the curve upwards.

Changes in hazard are not uniform across Queensland, as the changes in track behaviour are important for understanding the likelihood of TC occurrence at any given location. For example, the expansion of the tropical circulation means TCs are shifting polewards, reducing the frequency in the far north, but increasing the proportion of tracks that reach further south. There are also regional variations in the intensity distribution – some areas may see a greater proportion of intense TCs compared to current climate, though confidence in those variations is low. However, a consistent signal we see in these profiles is a reduction in frequency, which reduces the annual exceedance probabilities. In most areas, this reduced frequency outweighs any change in the distribution of intensity, leading to lower annual exceedance probabilities.

Overall, decreasing intensity is consistent with the trends in thermodynamic indices, which point to a decline in the maximum potential intensity of TCs in the Queensland and Coral Sea regions. This projection is counter to the more widely reported global trends in TC intensity which indicates a shift towards more intense TCs (Knutson et al., 2020). In light of this, it would be prudent to further investigate these changes with additional regional models.

For the **Gold Coast**, the hazard profiles for the Group 1 ensemble (top row, Figure 35) display a consistent signal of reduced frequency of TCs, but an increase in the proportion of intense TCs. By the end of century, the wind speeds at annual probabilities ‹10^{-3} are higher than for earlier time periods, which indicates the rarest storms will be more intense. Even though the annual probabilities where the increase in wind speed are low, this would still have substantial consequences for emergency management. Design criteria for buildings essential to post-disaster recovery specify a 1:2000 annual exceedance probability for cyclonic wind (Australian Building Codes Board, 2019), so a projected increase in the wind speeds would warrant an increase in the design specification for buildings used in support of response and recovery actions in the region.

Design loads for residential houses are determined around higher annual probabilities (0.02), where there is no increase in hazard evident that may initiate changes to construction standards. The implication is that emergency services may need respond to potentially more catastrophic events that exceed the bounds of building design criteria. This may also impact the design criteria for buildings used for post-disaster.

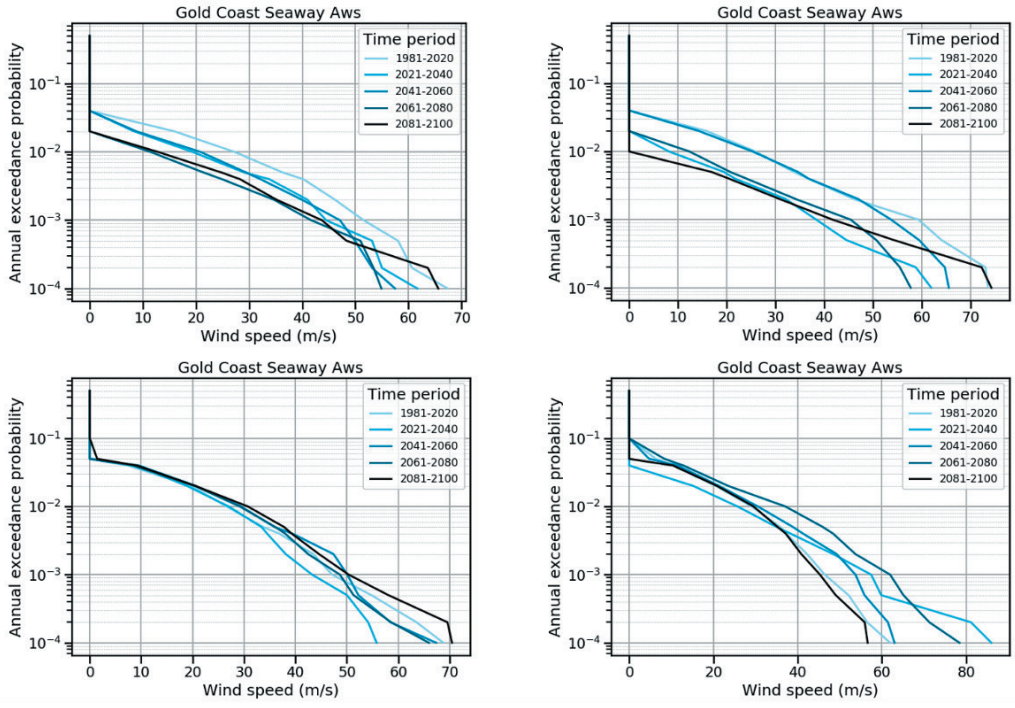

Figure 35: Annual exceedance probability curves for Gold Coast for Group 1, RCP4.5 (top left), Group 1, RCP8.5 (top right), Group 2, RCP4.5 (lower left) and Group 2, RCP8.5 (lower right). Note the different horizontal scales in each panel.

For both **Gladstone** (Figure 36) and **Mackay** (Figure 37), the reduced frequency dominates the changes in hazard profiles, evidenced by the downward translation of the hazard profiles for Group 1, RCP8.5 in each case (top right panel). There is no clear signal in the intensity distribution for these locations as the shape of the profile remains the same through all time periods.

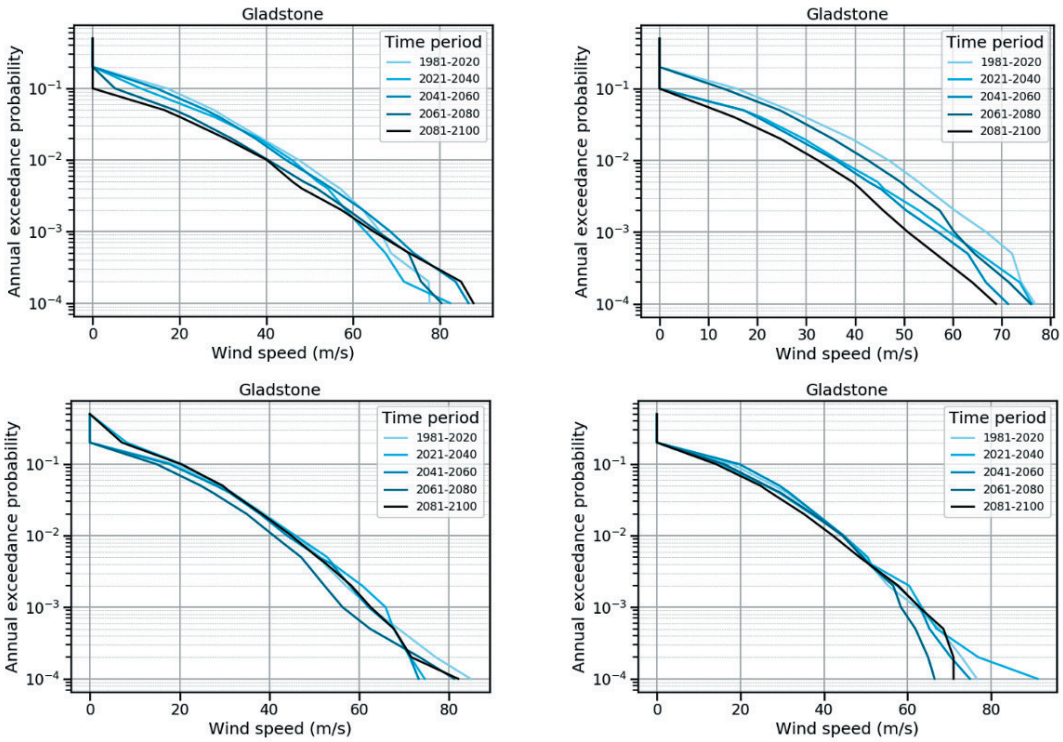

Figure 36: Annual exceedance probability curves for Gladstone for Group 1, RCP4.5 (top left), Group 1, RCP8.5 (top right), Group 2, RCP4.5 (lower left) and Group 2, RCP8.5 (lower right). Note the different horizontal scales in each panel.

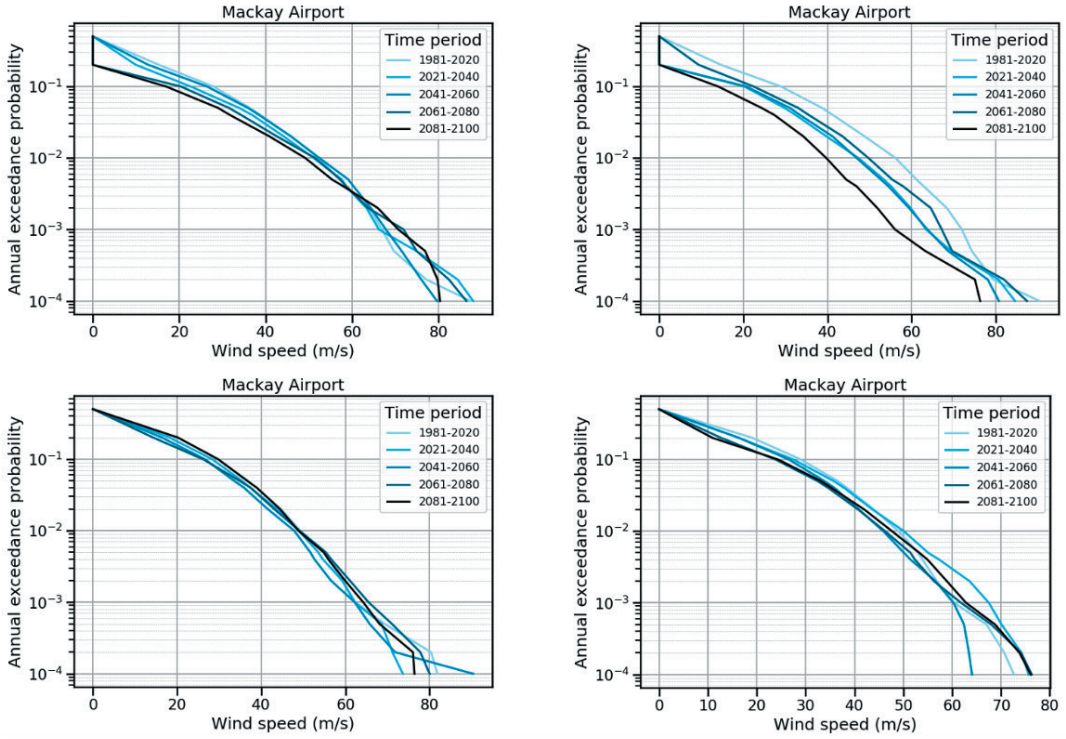

Figure 37: Annual exceedance probability curves for Mackay for Group 1, RCP4.5 (top left), Group 1, RCP8.5 (top right), Group 2, RCP4.5 (lower left) and Group 2, RCP8.5 (lower right). Note the different horizontal scales in each panel.

The **Townsville** AEP curves for RCP8.5 indicate an overall reduction in hazard by the end of the twenty-first century (Figure 38). The Group 1 ensemble indicates a reduction of over 10m/s (36km/h) for most exceedance probabilities. There is no discernible shift in the intensity distribution (i.e. change in the shape of the AEP curve). For Group 2, there is a slight reduction in hazard for the higher AEP range (AEP $>10^{-1}$), but essentially no change for AEP $<10^{-2}$.

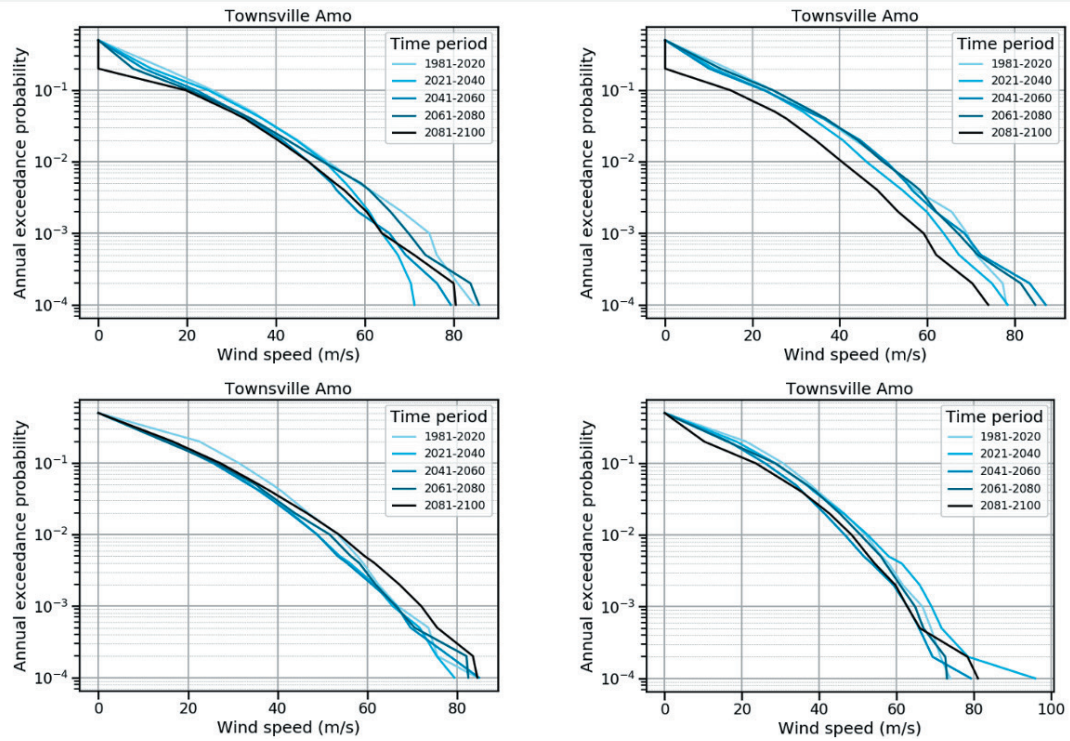

Figure 38: Annual exceedance probability curves for Townsville for Group 1, RCP4.5 (top left), Group 1, RCP8.5 (top right), Group 2, RCP4.5 (lower left) and Group 2, RCP8.5 (lower right). Note the different horizontal scales in each panel.

Both ensembles indicate a decrease in hazard for **Cairns** under RCP8.5, though the magnitude of the change is greater for Group 1 (Figure 39). As with Townsville, there is nearly 10m/s reduction in AEP wind speeds in the Group 1 ensemble and about 5m/s in Group 2. Again, there is no discernible change in the shape of the hazard profile, indicating there is not likely to be a change in the distribution of intensity of storms affecting Cairns, only a reduction in the frequency.

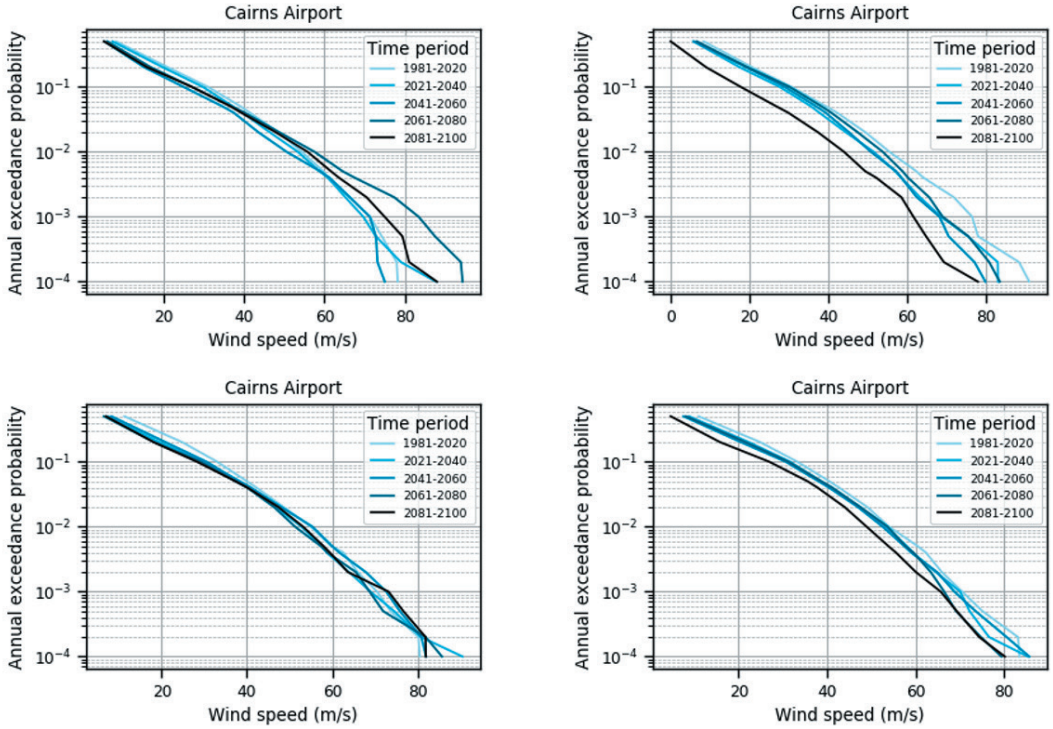

Figure 39: Annual exceedance probability curves for Cairns for Group 1, RCP4.5 (top left), Group 1, RCP8.5 (top right), Group 2, RCP4.5 (lower left) and Group 2, RCP8.5 (lower right). Note the different horizontal scales in each panel.

The hazard profile for **Kowanyama** (similarly for Pormpuraaw) shows virtually no significant trend towards the end of the century (Figure 40). There may be a weak trend towards a more intense distribution of TC intensity, with the Group 1 RCP8.5 scenario (top right, Figure 40) showing a slight flattening of the hazard profile through the future time periods.

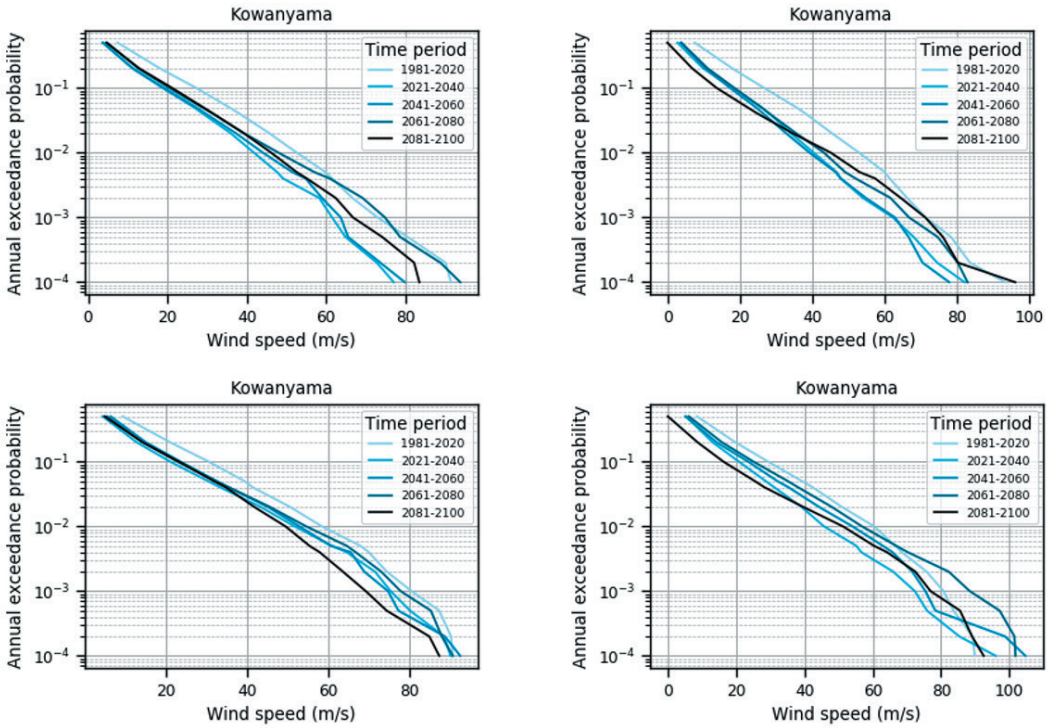

Figure 40: Annual exceedance probability curves for Kowanyama for Group 1, RCP4.5 (top left), Group 1, RCP8.5 (top right), Group 2, RCP4.5 (lower left) and Group 2, RCP8.5 (lower right). Note the different horizontal scales in each panel.

6 SUMMARY

6 Summary

More likely than not, some communities across Queensland will see an increase in the likelihood of extreme TC events into the future, but for most, the reduced annual frequency of TCs across North Queensland will see the AEP wind speeds reduced into the future. Most communities are unlikely to experience significant change in wind hazard at the 1:500 AEP level. This absence of significant change is unlikely to warrant changes to building design standards for residential housing. However, the one region likely to experience an increase in TC-related wind hazard is South East Queensland, where existing wind loading design standards for all buildings are lower than areas north of Bundaberg.

Modelled changes in the likelihood of severe events – especially in South East Queensland – should bring attention to the consideration of evacuation facilities and the building assets used for coordinating post-disaster recovery activities, to ensure they remain functioning in the event of a severe TC. The Building Code of Australia specifies a 1:2000 AEP for those structures essential to post-disaster recovery (Australian Building Codes Board, 2019), and there is evidence of an increase in wind speeds at these likelihoods over South East Queensland. There are also other studies investigating changes in TC activity over the Queensland region, which indicate an increase in the likelihood of more destructive cyclones affecting South East Queensland (Bruyère et al., 2020).

While the confidence in this result is low (given the shortcomings noted previously), it would be sensible to undertake a more detailed analysis of the changes, and the potential of increasing the design criteria for those buildings that support post-disaster recovery operations. Investment in upgrading those buildings used for post-disaster recovery activities would deliver increased resilience for the community, especially in South East Queensland where there continues to be the potential for severe TCs. Even at lower wind intensities, issues relating to water ingress impacting the functionality of the facility must be considered.

There remains uncertainty in the future change in TC frequency (the number of tropical cyclones in a given period) projected by climate models, with a general tendency for models to project fewer tropical cyclones in the Australia region in the future climate and a greater proportion of the high intensity storms (stronger wind speeds and heavier rainfall).

Wind speed is only one aspect of TCs and their impacts. The amount of heavy precipitation from all weather systems, including TCs, is likely to increase. Increased rainfall intensity from TCs is pertinent to Australia, since these storms have historically been associated with major flooding.

Additionally, increases in storm surges and extreme sea-levels are very likely to occur in association with TCs under future climate change. This change is independent of changes in TC intensity and is directly related to increases in global mean sea-level due to global warming.

Projected changes in TC characteristics are inherently tied to changes in large-scale patterns such as the El Niño - Southern Oscillation, changes in sea surface temperature and changes in deep convection. As global climate models improve, their simulation of TCs is expected to improve, thus providing greater certainty in projections of TC changes in a warmer world.

Further investigation into the changes of TC activity, especially around the intensity of events should be undertaken, given some of the shortcomings noted earlier in this section. The forthcoming Severe Wind Hazard Assessment for South East Queensland SWHA-SEQ will focus on that region, in collaboration with insurance industry partners, to draw together the body of knowledge on wind hazard projections under climate change. The SWHA-SEQ project is scheduled to report on this research in 2022. Additionally, climate change impacts on TC activity is a prominent area of climate research given the consequences of these events, and is advancing rapidly. Future generations of global circulation models and regional climate models will help to refine our understanding of the projected changes of TC frequency, tracks and intensity, and therefore the likelihood of extreme TC-related winds across Queensland. Further, future generations of wind hazard models will continue to evolve due to improved understanding of wind behaviour and additional observations.

7 References

Arthur, W. C., 2018: Tropical Cyclone Hazard Assessment: 2018 Release. Geoscience Australia Record, Record 2018/40, http://pid.geoscience.gov.au/dataset/ga/123412.

Arthur, W. C. (2021). A statistical–parametric model of tropical cyclones for hazard assessment. Nat. Hazards Earth Syst. Sci., 21(3), 893–916. https://doi.org/10.5194/nhess-21-893-2021

Arthur, W. C., Chesnais, M., Phillips, B., Martin, S., Wehner, M., Edwards, M., Henderson, D., Smith, D., Doolan, J., Trancoso, R., Syktus, J., Rice, M. and Poutinen, M. 2020. Severe Wind Hazard Assessment for Queensland: An evaluation of current and future tropical cyclone risk. Queensland Fire and Emergency Services, Brisbane. Geoscience Australia, Canberra. https://www.disaster.qld.gov.au/qermf/Pages/Assessment-and-plans.aspx.

Bruyère, C., B. W. Buckley, A. Prein, G. Holland, M. Leplastrier, D. J. Henderson, P. Chan, J. M. Done, and A. Dyer, 2020: Severe Weather in a Changing Climate, https://www.iag.com.au/severe-weather-changing-climate-2nd-edition.

Callaghan, J., and S. B. Power, 2011: Variability and decline in the number of severe tropical cyclones making land-fall over eastern Australia since the late nineteenth century. Climate Dynamics, **37**, 16.

Cannon, A. J., S. R. Sobie, and T. Q. Murdock, 2015: Bias Correction of GCM Precipitation by Quantile Mapping: How Well Do Methods Preserve Changes in Quantiles and Extremes? Journal of Climate, **28**, 6938-6959, 10.1175/jcli-d-14-00754.1.

CSIRO, and Bureau of Meteorology, 2015: Climate Change in Australia: Information for Australia's Natural Resource Management Regions: Technical Report. https://www.climatechangeinaustralia.gov.au/en/publications-library/technical-report/.

Dutheil, C., M. Lengaigne, M. Bador, J. Vialard, J. Lefèvre, N. C. Jourdain, S. Jullien, A. Peltier, B. Sultan, and C. Menkès, 2020: Impact of projected sea surface temperature biases on tropical cyclones projections in the South Pacific. Scientific Reports, **10**, 4838, **10**, 1038/s41598-020-61570-6.

Eccles, R., Zhang, H., Hamilton, D., Trancoso, R., & Syktus, J. (2020). Impacts of climate change on streamflow and floodplain inundation in a coastal subtropical catchment. *Advances in Water Resources*, 103825.

Hall, T. M., and S. Jewson, 2008: Comparison of Local and Basinwide Methods for Risk Assessment of Tropical Cyclone Landfall. Journal of Applied Meteorology and Climatology, **47**, 361-367.

Hall, T. M., and E. Yonekura, 2013: North American tropical cyclone landfall and SST: a statistical model study. Journal of Climate, **26**, 8422-8439.

Hoffmann, P., J. J. Katzfey, J. L. McGregor, and M. Thatcher, 2016: Bias and variance correction of sea surface temperatures used for dynamical downscaling. Journal of Geophysical Research Atmospheres, **121**, 12,877-812,890, 10.1002/2016jd025383.

Holland, G., and C. L. Bruyère, 2014: Recent intense hurricane response to global climate change. Climate Dynamics, **42**, 617-627.

Holland, G. J., 2007: Misuse of Landfall as a Proxy for Atlantic Tropical Cyclone Activity. Eos, **88**, 2.

Huang, P., and J. Ying, 2015: A Multimodel Ensemble Pattern Regression Method to Correct the Tropical Pacific SST Change Patterns under Global Warming. Journal of Climate, **28**, 4706-4723, 10.1175/JCLI-D-14-00833.1 %J Journal of Climate.

Knutson, T., S. J. Camargo, J. C. L. Chan, K. Emanuel, C.-H. Ho, J. Kossin, M. Mohapatra, M. Satoh, M. Sugi, K. Walsh and L. Wu, 2020: Tropical Cyclones and Climate Change Assessment: Part II: Projected Response to Anthropogenic Warming. Bulletin of American Meteorological Society, **101**, E303-E322, 10.1175/bams-d-18-0194.1.

Kossin, J. P., K. A. Emanuel, and G. A. Vecchi, 2014: The poleward migration of the location of tropical cyclone maximum intensity. Nature, **509**, 349-352.

Kossin, J. P., T. L. Olander, and K. R. Knapp, 2013: Trend Analysis with a New Global Record of Tropical Cyclone Intensity. Journal of Climate, **26**, 9960-9976, 10.1175/JCLI-D-13-00262.1.

Kriesche, B., H. Weindl, A. Smolka, and V. Schmidt, 2014: Stochastic Simulation model for Tropical Cyclone Tracks with Special Emphasis on Landfall Behavior. Natural Hazards, **73**, 335-353.

McGregor, J., and M. R. Dix, 2008: An Updated Description of the Conformal-Cubic Atmospheric Model. High Resolution Numerical Modelling of the Atmosphere and Ocean, K. Hamilton, and W. Ohfuchi, Eds., Springer, 51-75.

McInnes, K., R. Hoeke, K. E. Walsh, J. O'Grady, and G. Hubbert, 2015: Application of a synthetic cyclone method for assessment of tropical cyclone storm tides in Samoa. Natural Hazards, 1-20.

Nguyen, K.C., Walsh, K.J.E., 2001. Interannual, decadal, and transient greenhouse simulation of tropical cyclone-like vortices in a regional climate model of the South Pacific. Journal of Climate 14, 3043–3054. https://journals.ametsoc.org/view/journals/clim/14/13/1520-0442_2001_014_3043_idatgs_2.0.co_2.xml?tab_body=fulltext-display.

Nott, J., and M. Hayne, 2001: High frequency of 'super-cyclones' along the Great Barrier Reef over the past 5,000 years. Nature, **413**, 508-512, 10.1038/35097055.

Nott, J., S. Smithers, K. Walsh, and E. Rhodes, 2009: Sand beach ridges record 6000 year history of extreme tropical cyclone activity in northeastern Australia. Quaternary Science Reviews, **28**, 1511-1520, https://doi.org/10.1016/j.quascirev.2009.02.014.

Ogata, T., R. Mizuta, Y. Adachi, H. Murakami, and T. Ose, 2016: Atmosphere-Ocean Coupling Effect on Intense Tropical Cyclone Distribution and its Future Change with 60 km-AOGCM. Scientific Reports, **6**, 29800, 10.1038/srep29800.

Schwalm, C. R., S. Glendon, and P. B. Duffy, 2020: RCP8.5 tracks cumulative CO2 emissions. Proceedings of the National Academy of Sciences, 202007117, 10.1073/pnas.2007117117.

Siqueira, A., W. C. Arthur, and H. M. Woolf, 2014: Evaluation of severe wind hazard from tropical cyclones - current and future climate simulations: Pacific-Australia Climate Change Science and Adaptation Planning Program. Geoscience Australia Record, **47**, http://www.ga.gov.au/corporate_data/79681/Rec2014_047.pdf.

Thatcher, M., and J. L. McGregor, 2011: A Technique for Dynamically Downscaling Daily-Averaged GCM Datasets Using the Conformal Cubic Atmospheric Model. Monthly Weather Review, **139**, 79-95.

Trancoso, R., Syktus, J., Toombs, N., Ahrens, D., Wong, K. K. H., & Dalla Pozza, R. (2020). Heatwaves intensification in Australia: A consistent trajectory across past, present and future. Science of The Total Environment, **742**, 140521.

van Vuuren, D. P., J. Edmonds, M. Kainuma, K. Riahi, A. Thomson, K. A. Hibbard, G. C. Hurtt, T. Kram, V. Krey, J.-F. Lamarque, T. Masui, M. Meinshausen, N. Nakicenovic, S. J. Smith and S. K. Rose, 2011: The representative concentration pathways: an overview. Climatic Change, **109**, 5-31.

Walsh, K. J., & Syktus, J. (2003). Simulations of observed interannual variability of tropical cyclone formation east of Australia. Atmospheric Science Letters, 4(1-4), 28-40.

Walsh, K., S. Lavender, E. Scoccimarro, and H. Murakami, 2013: Resolution dependence of tropical cyclone formation in CMIP3 and finer resolution models. Climate Dynamics, **40**, 585-599, 10.1007/s00382-012-1298-z.

Walsh, K. J. E., 1997: Objective Detection of Tropical Cyclones in High-Resolution Analyses. Monthly Weather Review, **125**, 1767--1779, 10.1175/1520-0493(1997)125<1767:ODOTCI>2.0.CO;2.

Walsh, K. J. E., M. Fiorino, C. W. Landsea, and K. L. McInnes, 2007: Objectively Determined Resolution-Dependent Threshold Criteria for the Detection of Tropical Cyclones in Climate Models and Reanalyses. Journal of Climate, **20**, 2307-2314.

Walsh, K. J. E., K.-C. Nguyen, and J. L. McGregor, 2004: Fine-resolution regional climate model simulations of the impact of climate change on tropical cyclones near Australia. Climate Dynamics, **22**, 47-56.

Weinkle, J., R. Maue, and R. Pielke Jr., 2012: Historical Global Tropical Cyclone Landfalls. Journal of Climate, **25**, 4729-4735.

Zarzycki, C. M., 2016: Tropical Cyclone Intensity Errors Associated with Lack of Two-Way Ocean Coupling in High-Resolution Global Simulations. Journal of Climate, **29**, 8589-8610, 10.1175/JCLI-D-16-0273.1 %J Journal of Climate.

Appendix A: Acronyms

Abbreviation	Definition
RP	Return Period. *The average time between events of a given magnitude. For example, the average time between events with a maximum wind gust of 150 km/h or greater.*
ARI	Average Recurrence Interval. *As for return period – the average time between events of a given magnitude or greater.*
AEP	Annual Exceedance Probability. *The probability of an event of a given magnitude (or greater) occurring in any year. Can be expressed as either a probability with values ranging from 0 to 1, or as a percentage with a range from 0 to 100%.*
RCM	Regional Climate Model. *A numerical model that simulates atmospheric and land surface (and sometime ocean) processes over a region of the globe. These are forced by specified lateral and ocean conditions drawn from a general circulation model.*
TCLV	Tropical Cyclone-Like Vortex. *A feature of numerical models (including regional climate models) that displays characteristics of a tropical cyclone such as a closed low pressure centre, cyclonic vorticity positive mid-level temperature anomalies and low-level wind maxima (Walsh, 1997).*
GCM	General Circulation Model. *A numerical model that represents physical processes in the atmosphere, ocean, cryosphere and land surface to simulate the response of the global climate system to greenhouse gases and atmospheric pollutants.*
RCP	Representative Concentration Pathway. *A set of socio-economic and emission scenarios that describe how the future may evolve with respect to socio-economic change, technology, energy and land use and emissions of greenhouse gases and air pollutants. They are used as input for climate models to define the radiative forcing due to changing greenhouse gases and air pollutants (van Vuuren et al., 2011).*

Appendix B: Annual recurrence intervals and event probability

This section provides guidance on comparing average recurrence intervals, annual exceedance probabilities and what can be termed 'lifetime' exceedance probabilities. The lifetime exceedance probability is the probability of one or more exceedances of a given threshold over a period of time – for example the probability of one (or more) 100-year ARI event(s) over a 30-year lifetime. In this example, the probability of a 100-year ARI event (or 0.01 AEP) is 0.2603, or a 26.03% chance of occurring over a 30-year period.

Annual exceedance probability	0.0004	0.001	0.002	0.004	0.01	0.02	0.04	0.1	0.2
Average Recurrence Interval	2,500	1000	500	250	**100**	**50**	**25**	**10**	**5**
Time span	**Probability**								
1	0.0004	0.0010	0.0020	0.0040	0.0100	0.0200	0.0400	0.1000	0.2000
5	0.0020	0.0050	0.0100	0.0198	0.0490	0.0961	0.1846	0.4095	0.6723
10	0.0040	0.0100	0.0198	0.0393	0.0956	0.1829	0.3352	0.6513	0.8926
20	0.0080	0.0198	0.0392	0.0770	0.1821	0.3324	0.5580	0.8784	0.9885
25	0.0100	0.0247	0.0488	0.0953	0.2222	0.3965	0.6396	0.9282	0.9962
30	0.0119	0.0296	0.0583	0.1133	0.2603	0.4545	0.7061	0.9576	0.9988
50	0.0198	0.0488	0.0953	0.1816	0.3950	0.6358	0.8701	0.9948	1.0000
100	0.0392	0.0952	0.1814	0.3302	0.6340	0.8674	0.9831	1.0000	1.0000

Table 2: Probability of one or more events with a defined annual exceedance probability, given a specified time span.

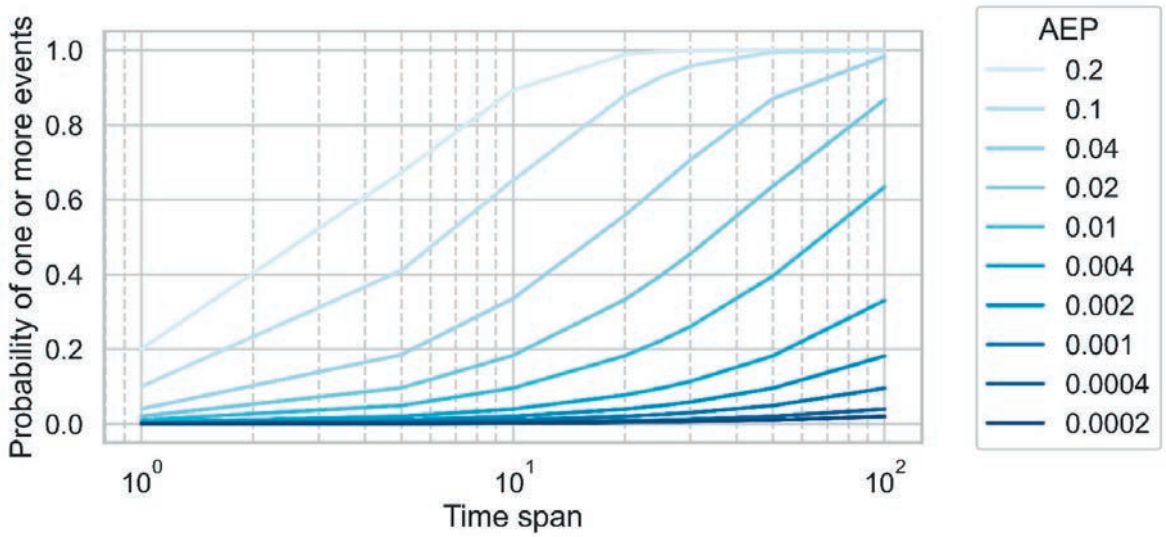

Figure 41: Probability of one or more events with a defined exceedance probability, given a specified time span for occurrence of events. For example, the probability of one or more events with an annual exceedance probability (AEP) of 0.01 (1%) in 50 years is 0.395 (39.5%).

Table 3 sets out the average recurrence interval for an event, where the likelihood of occurrence is defined for a defined time period. As an example, the residential wind loading design is based on a 10% probability of exceedance in a 50-year lifetime of a building. This translates to a 475-year average recurrence interval.

Probability	0.5	0.1	0.05	0.01	0.005	0.002
%	50	10	5	1	**0.5**	**0.2**
Time span	**Average recurrence interval**					
1	2	10	20	100	200	500
10	15	95	195	995	1,995	4,995
25	37	238	488	2,488	4,988	12,488
50	73	475	975	4,975	9,975	24,975
100	145	950	1,950	9,950	19,950	49,950
200	289	1,899	3,900	19,900	39,900	99,900
500	722	4,746	9,748	49,750	99,750	249,750
1000	1,443	9,492	19,496	99,500	199,500	499,500
2000	2,886	18,983	38,992	198,999	399,000	999,000

Table 3: Average recurrence intervals for events with a defined probability of occurring once in a given time span.

Appendix C: Likely impacts of near-future tropical cyclones on the Great Barrier Reef

Background

Day to day ('routine') wave energy plays a major role in shaping the geomorphology and ecology of coral reefs (Bradbury and Young 1981). TCs can generate waves that are considerably more energetic than what reefs typically experience and are thus beyond what reefs have adapted to absorb without damage. This damage ranges from minor (e.g. broken parts of colonies) to extreme (e.g. sand burial, dislodgement of massive colonies, destruction of entire reef structures) (Beeden et al., 2015).

Although reefs have evolved with cyclones over millennia, the combination of continued impacts from cyclone waves and the intensification of other stressors – particularly mass coral bleaching from thermal stress (Hughes et al., 2018) – is increasingly meaning that insufficient time is available for full recovery between events.

When reefs cannot fully recover, the cover of live coral may decline (see De'ath et al., 2012) and the future potential for recovery may be compromised. For example, on the Great Barrier Reef after three mass bleaching events in the past four years (2016, 2017 and 2020), coral communities have failed to regain past size class distributions (Dietzel et al., 2020) and functional trait diversity (McWilliam et al., 2020). This may result in changes to coral reefs that diminish the key ecosystem services they provide, such as shoreline protection (Ferrario et al., 2014) and fish habitat (Rogers et al., 2018).

While we cannot prevent or control cyclones, or coral reef response to them, understanding where and how often cyclone waves are likely to damage reefs is vital for planning management and conservation activities (Game et al., 2008; Beyer et al., 2018; Darling et al., 2019), for which disturbance dynamics is just one aspect of a complex decision-making challenge (Anthony et al., 2020). For example, it would not be prudent to focus reef restoration projects in areas likely to be damaged frequently by cyclones under current or near future climates.

The most damaging cyclones from a reef perspective are those that are strong, large in size and slow moving near reefs. The key question is whether climate scientists expect cyclones of these characteristics to occur more often near reefs.

- **Intensity:** There is general agreement that while a greater proportion of cyclones that form in future will be strong (see Bacmeister et al., 2018), cyclones overall may stay the same or drop in frequency (Walsh et al., 2015, Camargo and Wing, 2016 and noting Bhatia et al., 2018) due to an increase in inhibiting factors such as wind shear that make it harder for cyclones to form (Kang & Elser, 2015).

  This may or may not translate into more frequent strong cyclones near the Great Barrier Reef.

- **Size:** Little work has been done to predict how cyclone size may change in future climates (Walsh et al., 2016, Parker et al., 2018).

  Cyclone size makes a huge difference to the potential destructiveness of cyclones to reefs – but this remains largely unknown.

- **Forward speed:** Recent work raises the possibility that cyclones may move more slowly along their tracks as the climate warms (Zhang et al., 2020) and that cyclones may take longer to dissipate once they cross land (Li & Chakraborty, 2020).

  If the former is true for the Great Barrier Reef, this could maximise the wave heights that are possible for a given cyclone intensity because wave formation requires sufficient duration to reach fully developed seas. If the latter is true, this could increase the likelihood of cyclones reforming after crossing land.

- **Where they track:** How the spatial patterning and the form of the tracks themselves may change in future remains highly uncertain (Parker et al., 2018). Some evidence suggests that the location where cyclones reach their peak strength along their tracks has already moved poleward (Kossin et al., 2016), ranging from 7 (+/- 98) km per decade in the North Atlantic basin to 67 (+/- 55) km per decade in the South Indian basin.

  If this shift eventuates for the Great Barrier Reef, it should see a greater exposure of the far southern reef to damaging cyclone waves.

Project outline

To add to the understanding of how best to manage this, the Australian Institute of Marine Science (AIMS) in partnership with the Great Barrier Reef Marine Park Authority (GBRMPA) and the University of Queensland (UQ), and with assistance of the Department of Environment and Science (DES), undertook a project, as part of this Severe Wind Hazard Assessment for Queensland SWHA-Q, to characterise at fine spatial resolution (10 metre pixel) how the wave exposure risk to coral communities of the Great Barrier Reef from cyclones is likely to change from the current to the near future climate.

Specifically, the current climate is contrasted with an RCP4.5 and RCP8.5 scenario for a 2050 near future climate. A near future climate is used because coral reefs on average are expected to experience mass coral bleaching every year by 2054 (4.5 scenario) to 2043 (8.5 scenario) (van Hooidonk et al., 2016). Annual mass coral bleaching is expected to destroy most reefs (IPCC, 2018).

The Great Barrier Reef covers more than 340,000km^2 and includes more than 3,000 reefs. Given the computational demands that presents for numerical modelling at a 10m resolution, this report presents preliminary results for a case study of reefs to highlight what will be provided in due course via an academic journal paper and associated data repository.

The potential for severe wave damage to a given reef depends not just how high cyclone waves get, but also on how long waves capable of damaging reefs persist near that reef. Wave height and duration are a function of the intensity, overall size and forward speed of a cyclone; the greatest potential for damaging waves occurs for large sized cyclones that are strong and slow moving (Puotinen et al., 2016; Puotinen et al., 2020).

To account for this, the project had a dual focus. First, we used numerical wind and wave models (see Callaghan et al., 2020) to estimate the duration of threshold levels of significant wave heights (Hs – average height of top 1/3 highest waves recorded) approaching each reef pixel for a set of thousands of simulated cyclones for: i) current climate and ii) near future climate (2050) under a constrained (4.5 degrees) and aggressive (8.5 degrees) rate of warming.

The threshold Hs level (4m) corresponds to a sea state capable of causing severe reef damage, assuming vulnerable colonies are present (Puotinen et al., 2016). This was calculated for return intervals ranging from common (every 10 years) to rare (every 100 years). Second, for the same climate scenarios, we estimated the maximum significant wave height (Hs) expected for the same set of return intervals. We also calculated the extent to which wave energy approached each reef pixel from each of eight compass directions and assessed how the wave energy translated into indices of bottom stress.

For this report, we chose seven reefs that spanned the length (north to south) and breadth (inner, middle, outer continental shelf) to demonstrate the value of this data for understanding which reefs and parts of reefs are likely to be impacted by future cyclone waves and how often and how this differs from what happens under the current climate.

Once numerical modelling is complete for all 3,000 reefs of the Great Barrier Reef, we will do following:

- Characterise each reef into one of several groups based on its current and future cyclone exposure profile. For example, inner shelf reefs like Hook Island Reef have very low exposure now or in future and this is uniform across the reef. In contrast, outer shelf reefs in the far north like Yonge have very high exposure along a narrow band of their seaward edge but are quite sheltered on the lee side.
- For each reef and for each group above:
  - quantify the extent to which the dominant incoming wave direction(s) change at reefs in near future climates
  - quantify how exposure to peak Hs and duration of damaging waves changes.
- Assess whether exposure to cyclone wave energy shifts southward along the reef in the near future climate.

The resultant maps and statistics will highlight where reefs are most at risk from future cyclones which should be very useful for GBRMPA when planning management strategies, especially if combined with similar maps showing future risk from thermal stress and other stressors.

Project findings

The current climate

As shown in several previous studies (see Puotinen et al., 2016), reef exposure to cyclones along the Great Barrier Reef tends to be highest at the seaward sides of outer continental shelf reefs (Figure 42; Yonge Reef) and within central Great Barrier Reef from about Cairns to Rockhampton (Figure 42; Myrmidon Reef). In contrast, cyclone wave exposure tends to be lowest for inner shelf reefs (Figure 42; Hook Island Reef) and far northern inner and mid shelf reefs (Figure 42; Cockburn Reef).

Further, cyclone wave exposure is highly variable within individual reefs (Figure 42) and this is largely driven by the reef bathymetry (Figure 43) combined with the dominant incoming wave direction(s).

This happens because up to 95% of wave energy can be dissipated as waves encounter the complex three-dimensional structures of a given reef. This creates a 'wave shadow' within the reef with little exposure beyond the reef edge typically first encountered. This wave shadow can extend to create relatively sheltered conditions at reefs in the lee of the first reef reached by waves. As cyclone waves often approach the reef from seaward, this means the eastern edges of outer shelf reefs can be highly exposed (Figure 42; Yonge Reef) and how far wave energy penetrates depends on the spatial extent of the deeper reef slope (Figure 43: Yonge Reef). Thus, the maximum exposure of Yonge Reef is high but only covers a small percentage of the total area of the reef.

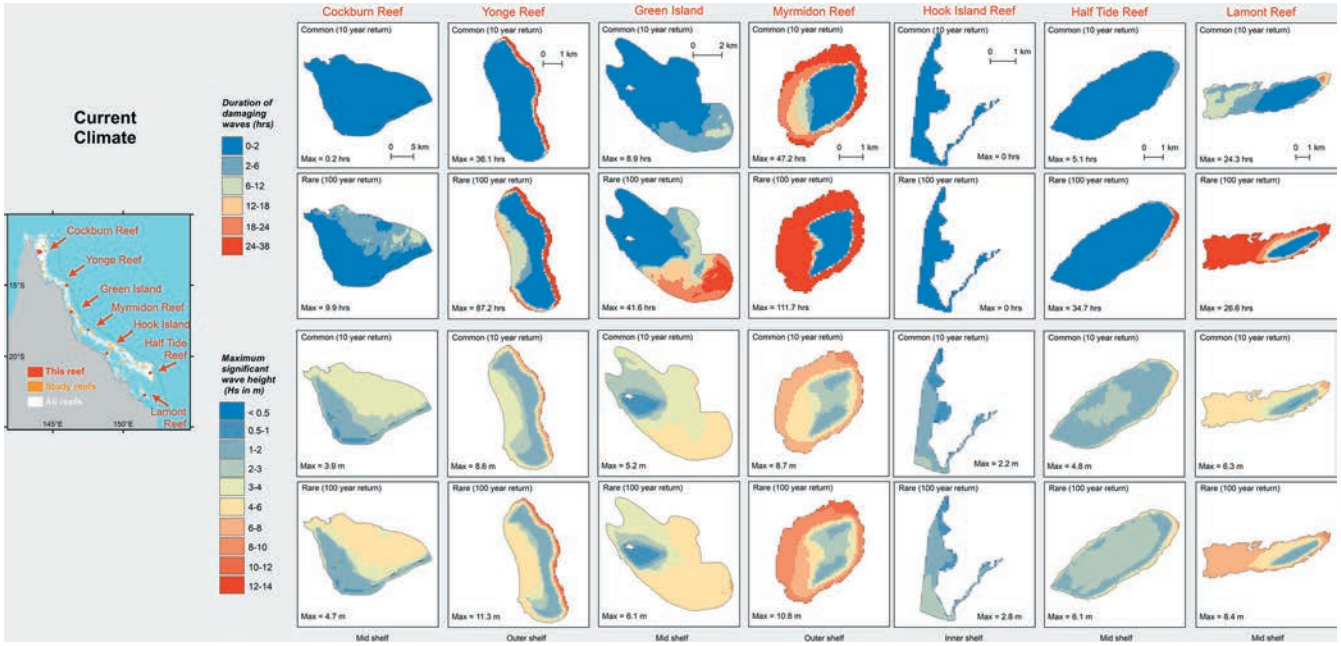

Figure 42: Great Barrier Reef modelled exposure to tropical cyclone generated waves under a current climate for seven reefs spanning the length (north to south) and breadth (inner, middle, outer continental shelf position) of the region. The top two rows show the modelled duration of waves capable of damaging most coral colonies under common conditions (10 year return period – top row) versus rare conditions (100 year return period – 2nd row). The bottom two rows show the modelled maximum significant wave height (Hs- average of top 1/3 highest waves) for common conditions (10 year return period – 3rd row) versus rare conditions (100 year return period – bottom row).

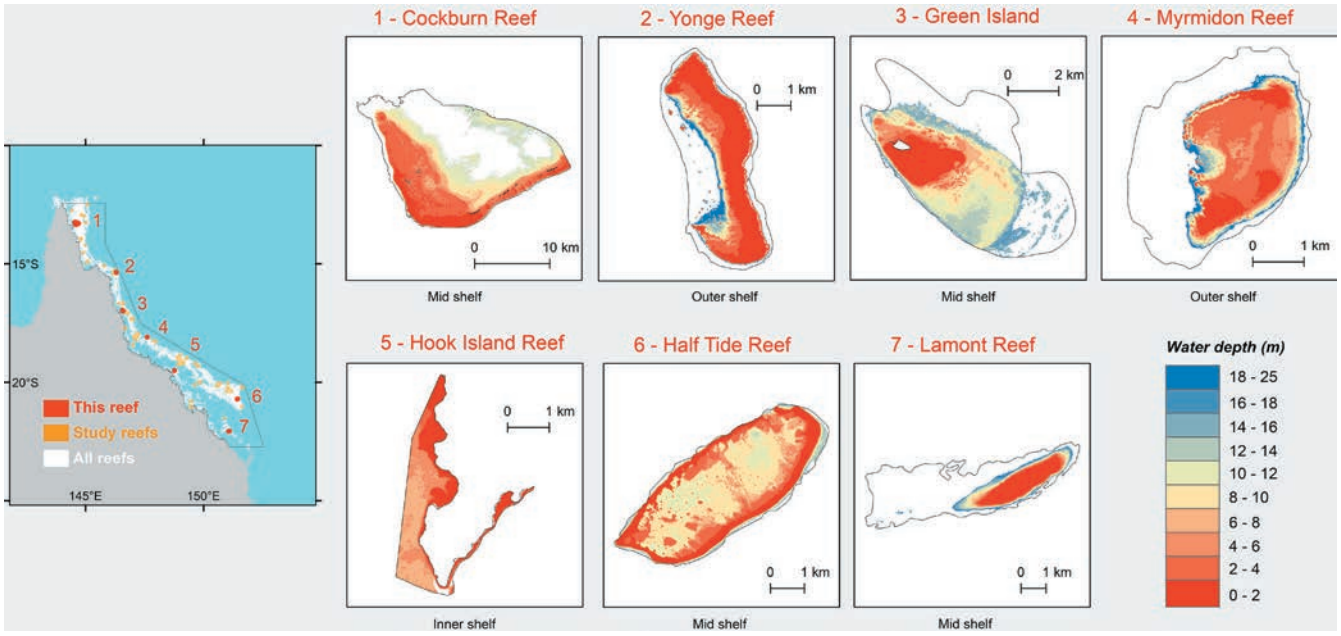

Figure 43: High resolution (10 metre) bathymetry data for seven selected reefs spanning the length (north to south) and breadth (inner, middle, outer continental shelf position) of the Great Barrier Reef used in numerical modelling of cyclone wave exposure.

Interestingly, for the seven case study reefs at least, most of the area of each reef did not differ much in the near future climate from the current climate for either the duration of damaging waves or the peak wave conditions (Figure 44). The greatest difference between the climates was always a drop in cyclone exposure in future (Figure 44; blue) although for the rare scenarios, some parts of Myrmidon Reef did see an increase. Interestingly, the southernmost case study reef (Figure 44; Lamont Reef) showed the most widespread drop in cyclone exposure. Whether this holds true in general will be revealed once numerical modelling is complete for all 3,000 reefs. If so, it highlights the fact that the distribution of cyclone wave energy is driven just as much by size and forward speed as by intensity – assuming that the near future climate shows strong cyclones further south than the current climate.

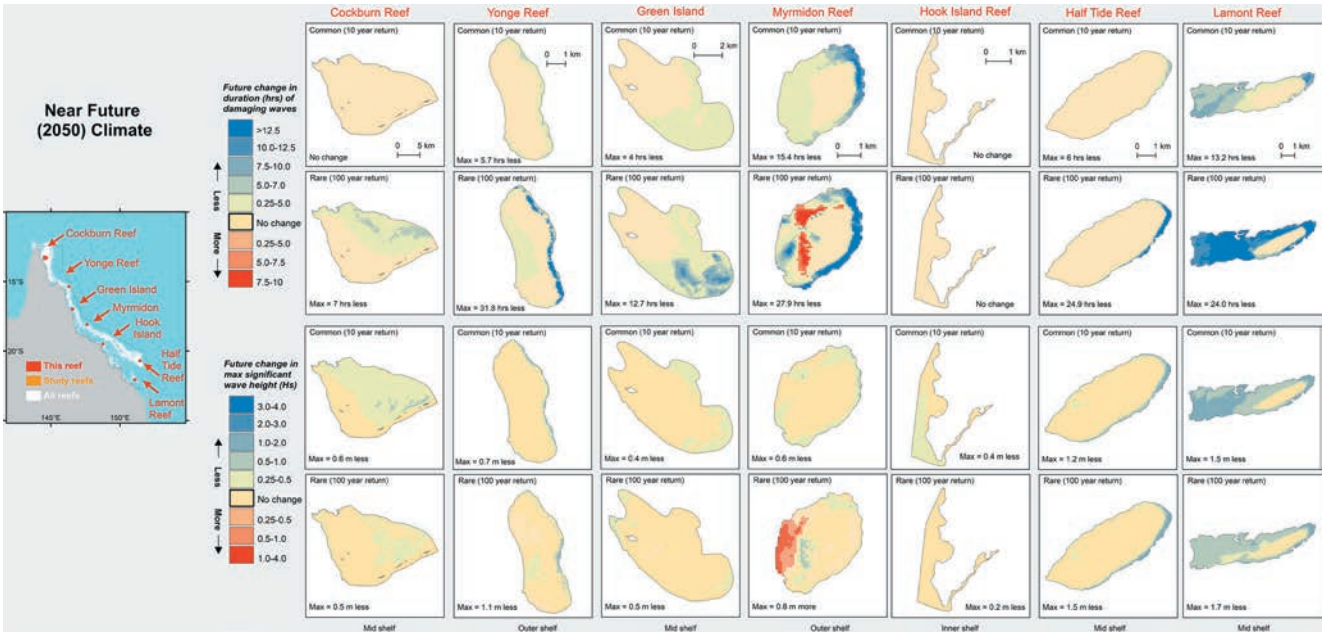

Figure 44: Great Barrier Reef modelled exposure to tropical cyclone generated waves under a near-future (2050) climate (8.5 degree scenario) for seven reefs spanning the length (north to south) and breadth (inner, middle, outer continental shelf position) of the region. The top two rows show the expected change in the modelled duration of waves capable of damaging most coral colonies under common conditions (10 year return period – top row) versus rare conditions (100 year return period – 2nd row). The bottom two rows show the expected change in the modelled maximum significant wave height (Hs- average of top 1/3 highest waves) for common conditions (10 year return period – 3rd row) versus rare conditions (100 year return period – bottom row).

Once the full analysis is complete, a repository of cyclone exposure data will be produced for each reef (as per Figure 45), and statistics calculated for the Great Barrier Reef as a whole and for each set of characteristic reefs (as previously described). This should prove invaluable for identifying which reefs and parts of reefs are and will be the most consistently exposed to damaging cyclone waves. GBRMPA and other research and management organisations can use this to help spatially prioritise conservation actions such as those proposed as part of the Reef Resilience and Adaptation Program (RRAP)[22].

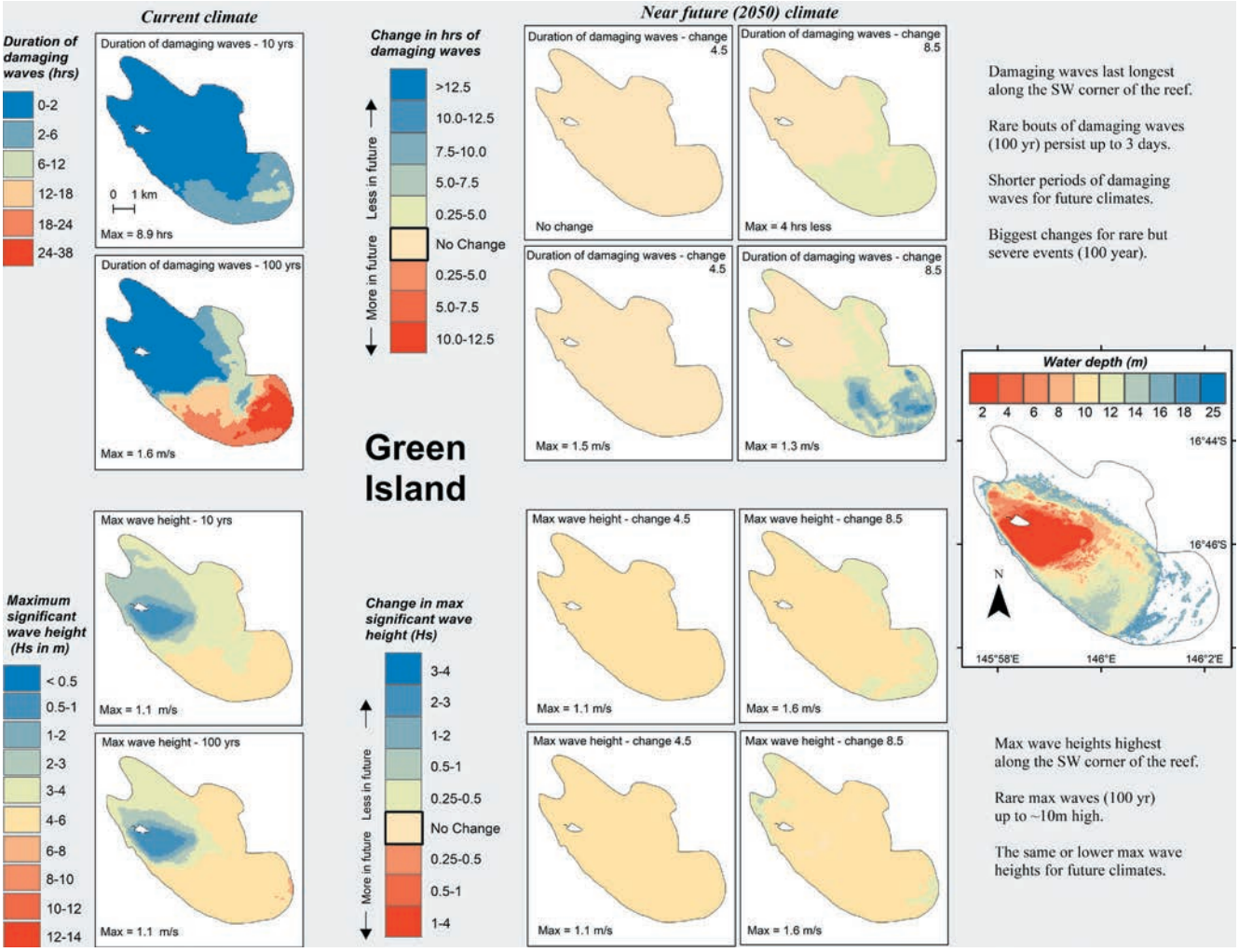

Figure 45: Summary of key project findings for an example reef (Green Island) to eventually be provided for all 3,000 reefs of the Great Barrier Reef in a follow-up paper from this project. It shows the current exposure to cyclone waves as per Figure 119, how this is expected to change as per Figure 121, and the depth profile of the reef as per Figure 123.

Final observations

In summary:

- **A rare opportunity for analysis**

  The unprecedented dataset produced by this project offers a rare opportunity to examine and compare cyclones from the past and near future from the perspective of the wave energy they generate between and within reefs.

- **A note of caution**

  The high spatial resolution and large set of synthetic cyclones implies a level of confidence that is not justified by the uncertainties that remain, particularly with regards to the spatial positioning of the tracks, how the regions of cyclogenesis are determined (which create notable spatial bias in where cyclones form and thus track), cyclone sizes (which make a huge difference to the spatial footprint of damaging waves) and the spatial and temporal patterns of where cyclones track.

- **How best to use it?**

  The project outputs are best used to explore the changes in exposure of the reef to damaging cyclone waves, given the assumptions of the climate models. Thus, the results represent one possible future, subject to considerable uncertainties (as previously noted).


BAKERS CREEK
KIRKUP BRIDGE

Queensland Government

Australian Government
Geoscience Australia

CYCLONE TESTING STATION

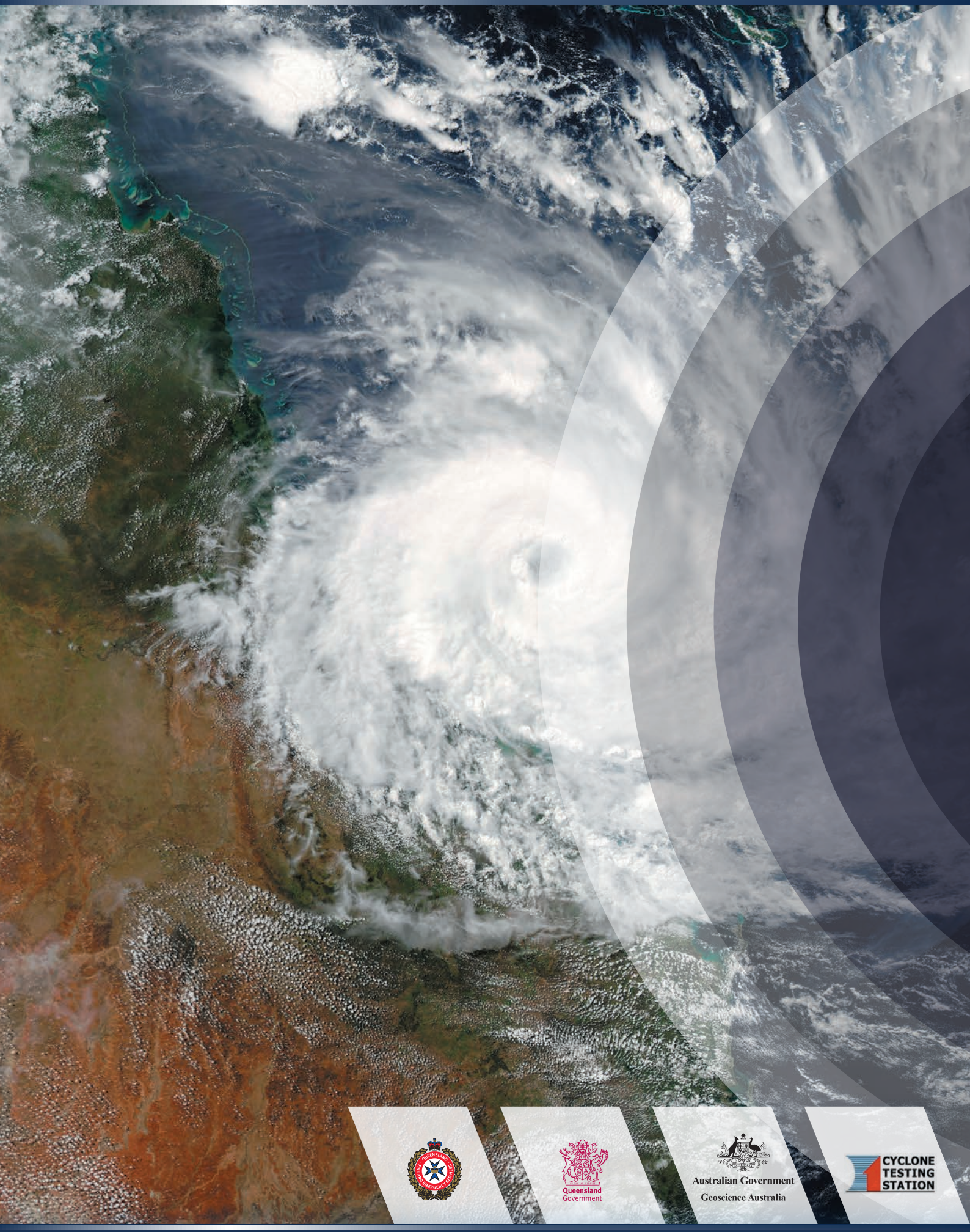

Queensland Government

Australian Government
Geoscience Australia

CYCLONE TESTING STATION

Severe Wind Hazard Assessment for Queensland TR2: Hazard assessment for future climate scenarios